Side peaks in Nb and NbTi point-contact spectra

Master's thesis
University of Turku
Department of Physics and Astronomy
Physics
2012
Jouko Huupponen
Referees:
Professor Kurt Gloos
Professor Kalevi Kokko

UNIVERSITY OF TURKU
Department of Physics and Astronomy

HUUPPONEN, JOUKO Side peaks in Nb and NbTi point-contact spectra

Master's thesis 42 p.
Physics
November 2012

Superconductor – normal metal point contacts were investigated, using different combinations of Cu, brass, Nb and NbTi. The resulting spectra contained side peaks. The currents at which these side peaks appeared, depended on the radii of the contacts. For contacts with Nb this dependence was quadratic, while for contacts with NbTi it was linear. Based on this, we argue that the side peaks in the case of the Nb contacts are due to the critical current density being exceeded. In contrast, side peaks of the NbTi contacts are caused by the self-magnetic field exceeding the lower critical field of NbTi. The NbTi contacts did not show the expected contribution from the vanishing Maxwell resistance of the superconductor, a question which remained open.

Keywords: Andreev reflection, Nb, NbTi, point contact, side peaks, superconductivity.

Contents

Introduction

Point contacts between normal metals and superconductors (S-N contacts) have been studied extensively for decades. The focus has been on ballistic point contacts, using materials with low electrical resistivities. In ballistic S-N point contacts a process called Andreev reflection governs the behavior of the contacts. Point contacts using materials with higher resitivities have gained less attention. The original motivation of this study was to compare measurements with metals, that have high (normal state) resistivities, to those with low resistivities, to try and see if the Andreev reflection process is still visible and resolvable in the previous case.

During the course of the measurements the focus shifted to the subject of side peaks, maxima in the differential resistance spectra often found in point contacts with superconductors. These side peaks were analyzed and a relation to contact size was found. The contribution to the spectra from the normal state resistivity of the disordered superconductor remained as the other major topic, but the results were inconclusive.

The first chapter covers some basic theory of point contacts and superconductors. The second chapter describes the experimental setup. The third chapter consists of the experimental results and their analysis. The final chapter contains discussion on the results of the previous chapter.

1. Theory

1.1 Point contacts

This section concerning point contacts, as well as section 1.3 concerning point contacts and superconductors, are both largely based on the book Point-Contact Spectroscopy by Yu. G. Naidyuk and I. K. Yanson [1].

A point contact can be defined as a small constriction through which a current can be driven. In the mid 1960s Yu. Sharvin [2, cited in 1 p1] used such a constriction to inject non-equilibrium electrons into a metal to study its Fermi surface. In 1974 I. K. Yanson [3, cited in 1 p9] showed that point contacts can be used for energy resolved spectroscopy, starting what is known as point-contact spectroscopy (PCS). As for

present applications of point contacts, one could mention the measurement of the spin polarization of ferromagnets [4] and the study of unconventional superconductors [5], using so called Andreev reflection spectroscopy.

There are a number of different ways to make a point contact [1, p41]. These range from simply pressing two wires together, to creating constrictions with thin films using nanolithography. The different ways of making point contacts all have their own benefits and drawbacks, but they can all be treated within the same theoretical framework. The single most important parameter in describing a point contact is its size or radius. Based on their radii, point contacts can be divided into three different categories: ballistic [1, p17], diffusive [1, p24] and thermal [1, p28].

A contact is ballistic, if the radius a of the contact is much smaller then the mean-free path l of the electrons driven through the contact. In a ballistic contact, electrons pass through the contact without scattering. This means, that the change in the energies of the electrons after they have passed through the contact, is equivalent to the applied bias-voltage. This in turn makes the theoretical treatment of ballistic contacts considerably easier than the other kinds of contacts. Most theoretical models assume the contact to be ballistic. Even in the absence of any scattering a ballistic contact still has a nonzero resistance. This is known as the Sharvin resistance

$$R_{\text{Sharvin}} = \frac{2R_k}{(a\,k_F)^2} \quad , \tag{1}$$

where $R_k = h/e^2 = 25.8\ \text{k}\Omega$ a constant known as von Klitzing resistance and k_F is the Fermi wavenumber of the material in question.

If the radius of the contact is of the same size or larger than the inelastic diffusion length of the electrons, the contact is thermal. The diffusion length Λ is related to the elastic and inelastic mean free paths, l_{el} and l_{in}, in the following manner

$$\Lambda = \sqrt{\frac{1}{3}\cdot l_{el}\cdot l_{in}} \quad . \tag{2}$$

In a thermal contact an electron will scatter inelastically within the contact and lose a part of its energy. This causes the theoretical treatment of such contacts to be a great deal more difficult than that of ballistic contacts. The resistance of a thermal contact is called the Maxwell resistance

$$R_{\text{Maxwell}} = \frac{\rho}{2a} \quad , \tag{3}$$

where ρ is the electrical resistivity of the material in question. In the case of heterocontacts, that is to say a contact between two different materials, the average resistivity should be used [1, p30]. Thermal contacts have an additional difficulty associated with them: The energy the electrons lose as they scatter ends up heating the contact. This is known as local heating. The amount by which the contact heats up depends on the applied voltage. The temperature T at the center of the contact is given by a formula derived by F. Kohlrausch [6, cited in 1 p29]

$$T^2 - T_{bath}^2 = \frac{V^2}{4L} \quad , \tag{4}$$

where T_{bath} is the bath temperature, V the applied bias voltage and L the Lorentz number. If one ignores the bath temperature and uses the theoretical value for the Lorentz number, the result is a linear dependence between contact temperature and voltage, where each mV of applied voltage raises the temperature of the contact center by 3.2 K. This means that even very modest bias voltages can result in considerable heating. There are some cases where local heating can be of interest, but in the majority of cases it is a serious problem, making thermal contacts that much more difficult to use.

In addition to the ballistic and thermal contacts there is an intermediate case of diffusive contacts. A contact is diffusive when the radius of the contact is larger than the elastic mean-free path of the electrons, but still smaller than the diffusion length. As the electrons are scattered in the contact area, formulas that assume the contact to be ballistic are no longer valid. As with the thermal contacts this makes the theoretical treatment of such contacts more difficult, but since the electrons maintain their energies there is very little or no local heating and energy spectroscopy can be done.

There is a general formula known as Wexler's formula [7, cited in 1 p26] for the resistance of a point contact

$$R = \frac{2R_k}{(a k_F)^2} + \beta \frac{\rho}{2a} \quad , \tag{5}$$

where β is a numerical factor close to unity. In practice β can be taken to be equal to 1.0 reducing the formula simply to a sum of the Sharvin and Maxwell resistances

$$R \approx \frac{2R_k}{(a k_F)^2} + \frac{\rho}{2a} \quad . \tag{6}$$

Because of the different powers of the radius in the two terms, the Sharvin resistance dominates with small contacts and the Maxwell resistance with large contacts. What is

considered small or large depends primarily on the resistivity of the material since the Fermi wave numbers of different materials have less variation to them (at least for simple metals).

1.2 Superconductors

This section concerning superconductivity is based largely on the book Introduction To Superconductivity by M. Tinkham [8]

Superconductivity is a phenomena where a material loses its electrical resistivity and completely expels the magnetic field from within itself. This is caused by the electrons near the Fermi-surface joining together into pairs. This pairing is a result of phonons in the lattice creating an attractive force between two electrons, which at sufficiently low temperatures is enough to overcome the repulsive Coulomb force between the two electrons. Such a pair is known as a Cooper pair.

Near the Fermi-surface, where the electrons form Cooper pairs, a gap appears in the electron density of states. In this gap excitations of individual electrons are not stable and the electrons can only persist as parts of a Cooper pair. The existence of this gap is important to the Andreev reflection process described in section 1.4.

Superconductivity requires low temperatures. The temperature below which a material becomes superconducting is called a critical temperature, T_c. There is also a critical magnetic field, B_c. Superconductors can be divided into two groups based on their critical fields [8, p11]: type I that have a single critical field and type II that have two critical fields. In type I materials, when the magnetic field exceeds the critical field, the superconductivity is completely destroyed, in much the same way as if the critical temperature had been exceeded. Type II materials have two different critical fields: a lower critical field, B_{c1}, and a higher critical field, B_{c2}. When the lower critical filed is exceeded, the magnetic field begins to penetrate into the material, forming normal state regions known as vortices. The rest of the material remains superconducting, but as the magnetic field is increased more vortices begin to appear. When the magnetic field reaches the upper critical field the vortices fill the entire sample and superconductivity is completely destroyed.

There is also an additional critical field known as the thermodynamic critical field, $B_{c,th}$. For type I superconductors this is simply the same as the critical field B_c. For the type II superconductors, it is somewhere between the two critical fields. It can be approximated as the geometric average of the two other critical fields [8, p154]

$$B_{c,th} \approx \sqrt{B_{c1} \cdot B_{c2}} \quad . \tag{7}$$

1.3 Point contacts with superconductors

When one of the electrodes used in a point contact is a superconductor, ballistic, diffusive and thermal contacts are affected differently. In a ballistic contact superconductivity manifests itself in a process known as Andreev reflection [9]. This is the subject of section 1.4 below. In a thermal or diffusive contact there is an additional contribution from the vanishing electrical resistivity of the superconductor. If the superconductor has a high normal state resistivity this effect can be very large. Additionally, if the current driven through the point contact is sufficiently high, the superconductivity can be weakened or destroyed. Below three different ways are given, in which this can happen.

Current flowing through the contact will create a magnetic field. If this field, known as the self-magnetic field B_{sf}, exceeds the critical field B_c of the superconductor there should be a change in the behavior of the contact as the superconductor (or a part of it) becomes normal . Assuming the contact is circular one can derive a formula for the critical current when $B_{sf} = B_c$ [1, p216]

$$I_C = \frac{2\pi a B_c}{\mu_0} \quad , \tag{8}$$

where I_c is the critical current, a the radius of the contact, B_c the critical field of the superconductor and μ_0 the vacuum permeability. According to the above formula, the critical current depends linearly on the radius of the contact, or for a ballistic contact on the inverse of the square root of the resistance.

Another way in which the superconductivity can be destroyed, is if the current density exceeds the pair-breaking current density of the superconductor. At the pair-breaking current density the kinetic energy of the Cooper pairs exceeds the condensation energy of the pairs and the pairs are broken up, thus causing the superconductor to become

normal. The formula for the pair-breaking current density is [8, p124]

$$j_c = \frac{4 B_{c,th}}{3\sqrt{6}\mu_0 \lambda_L} \quad , \tag{9}$$

where j_c is the current density, $B_{c,th}$ is the thermodynamic critical field and λ_L is the London penetration depth of the superconductor. As the critical parameter is the current density the critical current scales with the area, that is to say, with the square of the radius of the contact. With a ballistic contact this means scaling inversely with the resistance of the contact.

Finally if the contact is thermal, local heating will play an important role. When the temperature of the contact reaches the critical temperature, the superconductor becomes normal in the contact region. In an N-S contact the (normal state) resistivities of both the superconductor and the normal metal, can cause local heating since the electrons are injected for the most part with energies outside of the energy gap. Local heating does not have a radius or a current dependence, it should only depend on the applied voltage and whether the contact is thermal.

There is one more phenomenon, the proximity effect, associated with superconductivity, that can affect a point contacts conductivity. When a superconductor is brought into close proximity with a normal metal, it is possible for a thin layer of the normal metal to become superconductive [10 p1005]. The superconductivity in the newly formed layer is often weaker and more easily destroyed than in the actual superconductor. This positive proximity effect, where the normal metal becomes superconductive, can be thought of as being caused by the Cooper pairs leaking into the normal metal. There is also a negative proximity effect, where a thin layer of the superconductor becomes normal or the superconductivity is weakened.

1.4 BTK-model

Presented by Blonder, Tinkham and Klapwijk in 1982, the BTK-model [11] is nowadays the standard model used to describe a ballistic point contact between a normal metal and a superconductor (N-S contact). In such contacts the normal current is converted into a supercurrent through the Andreev reflection (AR) process, where a Cooper pair is formed and a hole is reflected. The reflected holes contribute to the net current, and in the ideal case the AR process doubles the conductivity of the contact. The BTK-model

takes the AR process and adds the effects of a finite temperature and a non-zero interface barrier, allowing one to calculate the current-voltage characteristics of an N-S contact for a given set of parameters.

When an electron arrives at an N-S interface, it can be transmitted, normally reflected or Andreev reflected. A transmitted electron simply passes through the contact and contributes its charge to the total current. A normally reflected electron returns to the side from which it came from. In AR an electron coming from the normal side is transmitted into the superconductor where a Cooper pair is formed. Due to conservation laws a hole of opposite spin, momentum and energy (with respect to the chemical potential of the superconductor) is created. The hole follows the trajectory along which the electron has moved, only in the opposite direction. In this way the electron can be thought of as being reflected as a hole.

The BTK-model provides the probabilities for each of the three different processes by matching the slopes and magnitudes of the wave functions across the interface. These probabilities depend on the energy of the incident electron, the applied bias voltage, the size of energy gap and the strength of the interface barrier. Combining the probabilities with the assumption, that the occupation of electron states is given by an equilibrium Fermi function offset by the bias-voltage, the BTK model gives an expression for the current through the contact as a function of voltage. The use of the equilibrium Fermi functions limits the model to ballistic contacts. The result is a very distinctive double minimum structure in the differential resistance spectrum; minima on both sides of zero-bias at voltages corresponding to the energy gap and a maximum at zero-bias due to normal reflection from the interface barrier.

In the original form of the BTK-model there are three parameters that can be varied in order to produce a fit into experimental data: temperature, gap size and barrier strength. Temperature enters through the Fermi-distributions and has the effect of smearing the spectra, but it is not really an adjustable parameter, since it should be fixed at the bath temperature. The gap size determines the positions of the two minima. Since the gap size can differ from the bulk value, it should be treated as a variable parameter. The barrier strength, referred to as the Z parameter, dictates the size of the maximum at zero-bias. The Z parameter is essentially an empirical parameter intended to describe a complicated situation.

The BTK-model can be modified to take into account the effects of spin polarization in the normal metal [4] and the finite lifetime of the Cooper pairs [12]. The drawback is that instead of two parameters, namely the gap size and the *Z* parameter, one needs three or four parameters to describe the contact. The spin polarization has the effect of reducing the depths of the minimums as it hinders the AR process, but this effect can be avoided by using normal metals with no spin polarization. The finite lifetime has the effect of reducing both the depth of the minima and the height of the zero-bias maximum as well as changing the apparent width of the gap. Furthermore it is possible for the measured spectra to have backgrounds, that need to be accounted for before applying any form of the BTK-model. All this means that, while using the BTK-model itself is quite straightforward, reality can easily get difficult.

1.5 Disorder

There are two major contributors to the resistivity of a material: scatterings from phonons and scatterings from lattice defects. The phonon contribution depends strongly on the temperature whereas the lattice defects give a constant contribution independent from the temperature. As point contact measurements are generally made at very low temperatures, the resistivity in such experiments is primarily caused by the lattice defects, at least near the zero bias. At higher voltages electron phonon scatterings can begin to contribute to the resistance [1, p9].

To gauge the amount of lattice defects (disorder) in a sample, a figure known as a residual resistance ratio or RRR is used. RRR is defined as the resistance of the sample at room temperature divided by its resistance at a very low temperature (usually at 4.2 K, the temperature of liquid helium). It should be noted that an RRR value is specific to a particular sample, not a material itself. Samples with a high RRR are of high purity and have low electrical resistivities at low temperatures. Samples with low RRR are either simple metals of low purity or alloys, and they have higher electrical resistivities at low tempeatures.

The most obvious way in which disorder affects Andreev reflection, is though the possible addition of a Maxwell contribution to the resistance. There is also a model which adds a diffusive layer into the contact to simulate the disorder of the material [13]. This diffusive layer alters the shape of the differential resistance spectrum of the

contact, but as the model is somewhat more complicated than the standard BTK model and an existing computer program for the fitting was not available, this model is not used in this work.

2. Experimental methods

2.1 Fabrication of point contacts

As was previously mentioned there are several methods for fabricating point contacts. The two methods used in this study were the spear-anvil method, where a sharp needle is pressed against a plate, and the shear method, where two wires are slid against one another before a contact is made. For the measurements, that were made at constant temperature of 4.2 K, the samples were placed at the end of a dipstick, which was submerged in liquid helium. The point contact could be closed and opened by turning a steel wire that ran through the dipstick.

For the spear-anvil contacts turning the steel wire rotated a plate onto which a wire of one of the sample materials was soldered. One end of the wire had been cut so that it had a sharp angle to it. As the plate was rotated the sharp end of the wire was pressed against a plate made of the other sample material, forming the point contact. For the shear type contacts two wires were soldered in place in such a way that turning the steel wire caused the two sample wires to slide against one another, again forming the point contact. Figure (1) shows the setup for the shear type contacts.

For the measurements where the temperature was varied, the setup was slightly different as the samples had to be placed into the cryostat, meaning that the dipstick mentioned above could not be used. The cryostat had its own system for creating the point contact: the samples were connected with screws to sample holders that had been glued onto opposite ends of a bending plate. The plate could then be bent by turning a screw underneath it. As the plate bent, the sample holders tilted in opposite directions and the wires connected to them touched each other, creating a shear type point contact. Figure (2) shows this setup. The reason why the contacts were formed with this slightly unusual method, was that the cryostat had been used to make break-junction measurements, and this method requires very little modification to the setup. Despite the

Figure 1. A photo of the shear type point contact setup used in the dipstick. The rotating plate, that is used to open and close the contact, is to the right (not shown).

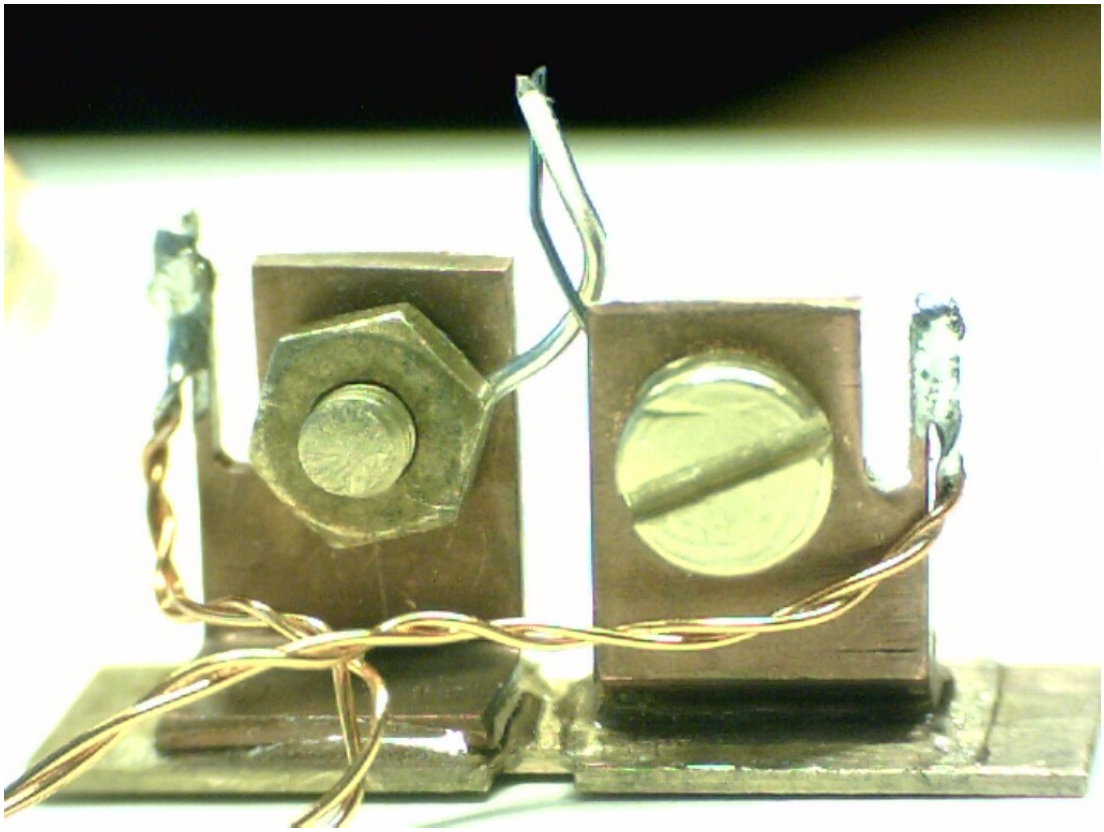

Figure 2. A photo of the point contact setup used in the dilution refrigerator. As the bending plate (bottom part) is bent, the two sample wires in the center of the figure move closer together and form the point contact.

somewhat unusual way in which they were created the contacts were actually quite stable.

2.2 Cryogenic systems

As was mentioned, the constant temperature measurements were done with the samples submerged in liquid helium. This way the sample is in good thermal contact with the liquid helium that is slowly boiling off. As long as the helium level stays above the sample, one can be sure that the sample temperature (excluding possible local heating) remains at 4.2 K, the boiling temperature of helium.

A dilution refrigerator was used for the measurements of the temperature series. It works by pumping a mixture of two helium isotopes, helium-3 and helium-4 [14, p149]. While dilution refrigerators can reach temperatures as low as 2 mK, for this work the samples were cooled only slightly below 1 K. The actual measurement temperature was controlled with a heater.

The cooling power of the refrigerator was not altered (except for how the cooling power of the refrigerator is reduced as the temperatures are lowered), instead a computer controlled system was used to drive a current through a resistor to heat the sample holder. When the temperature of the sample holder rose above the desired temperature the heating current was reduced, causing the temperature to start dropping. After the temperature had then dropped below the desired value the heating current was increased, so that eventually the temperature stabilized at the desired value. The temperatures were measured with a calibrated RuO_2 resistor.

Before measuring any temperature series, the contacts were repeatedly heated from 1 K to 11 K and cooled back to 1 K. Only after the spectra from two consecutive pairs of 1 K and 11 K measurements were identical were the actual temperature series measured. This was done to make sure the heating did not cause the contacts to change during the measurements of the temperature series, making sure that it was indeed the same contact being measured at different temperatures (strictly speaking it is possible that the contacts did chance, but in a reversible manner, but such behavior does not seem likely).

With some of the low resistance contacts, Joule heating became an issue. The low

resistances resulted in large currents at the higher bias-voltages, which in turn caused large amounts of Joule heating. Because of this the temperature controller was unable to keep the temperature stable. The problem was easily solved by limiting such measurements to lower bias-voltages, but as a result one of the temperature series ended up missing its 1 K measurement, as the voltage range that could be measured with the temperature still stable was too small.

2.3 Measurement system

The measurements were done with a four-terminal setup, so two pairs of electrical connections were made to the samples. One was used for current injection and the other for measuring the voltage drop across the contact and the differential resistance. The current injection was done with a voltage sweep conducted by the measurement computer via an analog-to-digital converter (ADC) system. In series with the point contact being measured was a reference resistor with a resistance several orders of magnitude higher than that of the contact. This way the resistance of the circuit was dominated by the constant resistance of the resistor and the voltage sweep of the entire circuit became a current sweep as far as the point contact itself was concerned. With the current sweep done in this manner, there was no need for any actual current measurements. All the measurements were voltage measurements.

The voltage drops over the contacts were measured in order to produce the I-V curves of the contacts and to be able to plot the differential resistances as functions of voltage. The differential resistances were measured with a lock-in amplifier. An external frequency generator was used to add a small AC signal into the injected current. The differential resistance spectra were recorded by using the output of the frequency generator as the reference signal for the lock-in amplifier. Before being recorded or sent to the lock-in, the voltage signals were amplified with a low-noise differential amplifier.

3. Results and analysis

3.1 Materials studied

To study the effects of disorder on normal-superconductor (N-S) point contacts, several series of measurements were made. For the normal electrodes Cu and brass were used.

Cu is an ordered metal (in these measurements a polycrystalline sample was used) and brass is an ordered alloy of Cu and Zn. For the superconducting electrodes Nb and NbTi were used. Here Nb is an ordered metal and NbTi is a disordered alloy of Nb and Ti. This results in four different pairings: Cu with Nb, Cu with NbTi, brass with Nb and brass with NbTi. Additionally a series of superconductor-superconductor (S-S) contacts were measured using a NbTi-NbTi pairing.

Cu and Nb are both metals that are often used in point contact experiments since they have low electrical resistivities (in the normal state for Nb), and are generally rather easy to work with. Furthermore the critical temperature of Nb is around 9.2 K [15], meaning it is well in the superconducting state at 4.2 K, the boiling temperature of liquid helium. Both brass and NbTi, when compared with Cu and Nb, have high electrical resistivities, so high that the resistivities of Cu and Nb can be ignored at low temperatures. While NbTi has essentially the same critical temperature as Nb (see fig. (3) below), it is a type II superconductor and has a much higher upper critical field.

The brass sample was a wire with a diameter of 0.33 mm, from the university workshop. Its exact composition was unknown. It had an RRR of 3.4 and a resistivity of 3.2 μΩcm at 4.2 K. The other samples were wires with diameters of 0.25 mm, from various commercial suppliers. The NbTi sample was a single core wire as opposed to the multifilament wires commonly used in practical applications. Its resistivity and the upper critical fields at different temperatures were measured with the PPMS (Physical property measurement system) magnetometer in the Wihuri lab. Figure (3) shows the results. It had an RRR of 1.2 and resistivity of 98 μΩcm at 10K, just above the transition. The critical magnetic field at 4.2 K was estimated to be around 12 T, a value that agrees with literature values [16]. The Cu and Nb samples had RRRs of 330 and 89. Their resistivities were not measured, but based on well-known literature values for the room temperature resistivities [15, p8] and the RRRs, they had resistivities of 0.0047 μΩcm and 0.17 μΩcm.

3.2 Sizes of the contacts

With eq. (1), (3) and (6) together with the resistivities and Fermi momenta of the materials, one can estimate the Sharvin, Maxwell and total resistances of contacts as functions of their radii. The resistivities are easy to measure and are given in the

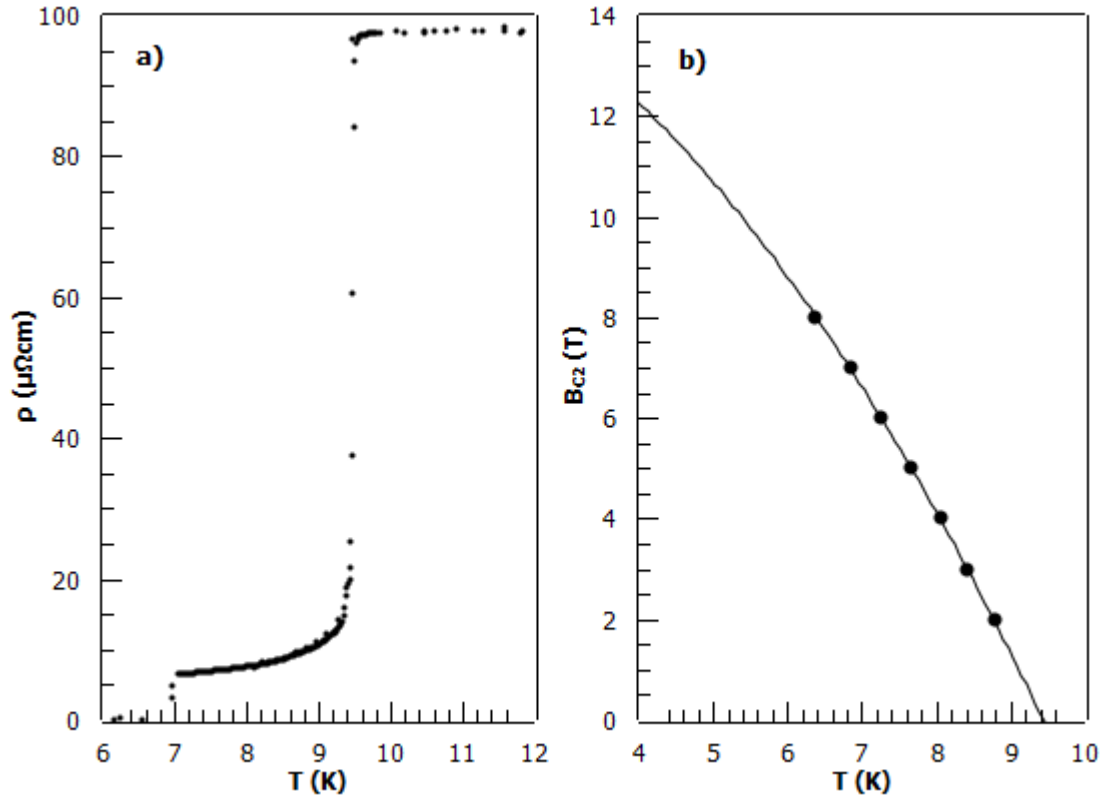

Figure 3. a) The resistivity of the NbTi sample as function of temperature. The critical temperature, where the transition happens, is roughly the same as the 9.2 K of Nb. The finite resistivity below the transition is probably caused by bad contacts. b) The critical fields of the NbTi sample at different temperatures extrapolated with a square fit to estimate the value at 4.2 K.

previous section. The Fermi momenta are a more difficult matter. They are not easy to measure and the literature values are often inconsistent. For the purpose of making some kind of estimate, the average of the theoretical values for Nb and Cu [15, p38] is used for all the metals. This gives a Fermi momentum of $1.27 \cdot 10^8$ 1/cm.

Figure (4) gives the Sharvin, Maxwell and total resistances, as functions of contact radius for the different pairings. The following resistivities were used: for Cu-Nb half of the Nb resistivity, for brass-Nb half of the brass resistivity, for Cu-NbTi and brass-NbTi half of the NbTi resistivity and for NbTi-NbTi the full NbTi resistivity. The contacts had resistances ranging from below one Ohm to several hundreds of Ohms. As is to be expected, the Cu-Nb pairings are almost entirely ballistic. With the brass-Nb pairings, the resistance was predominantly Sharvin resistance, making those contacts mostly ballistic. For the other pairings the resistance was mostly Maxwell resistance, making the contacts diffusive or thermal.

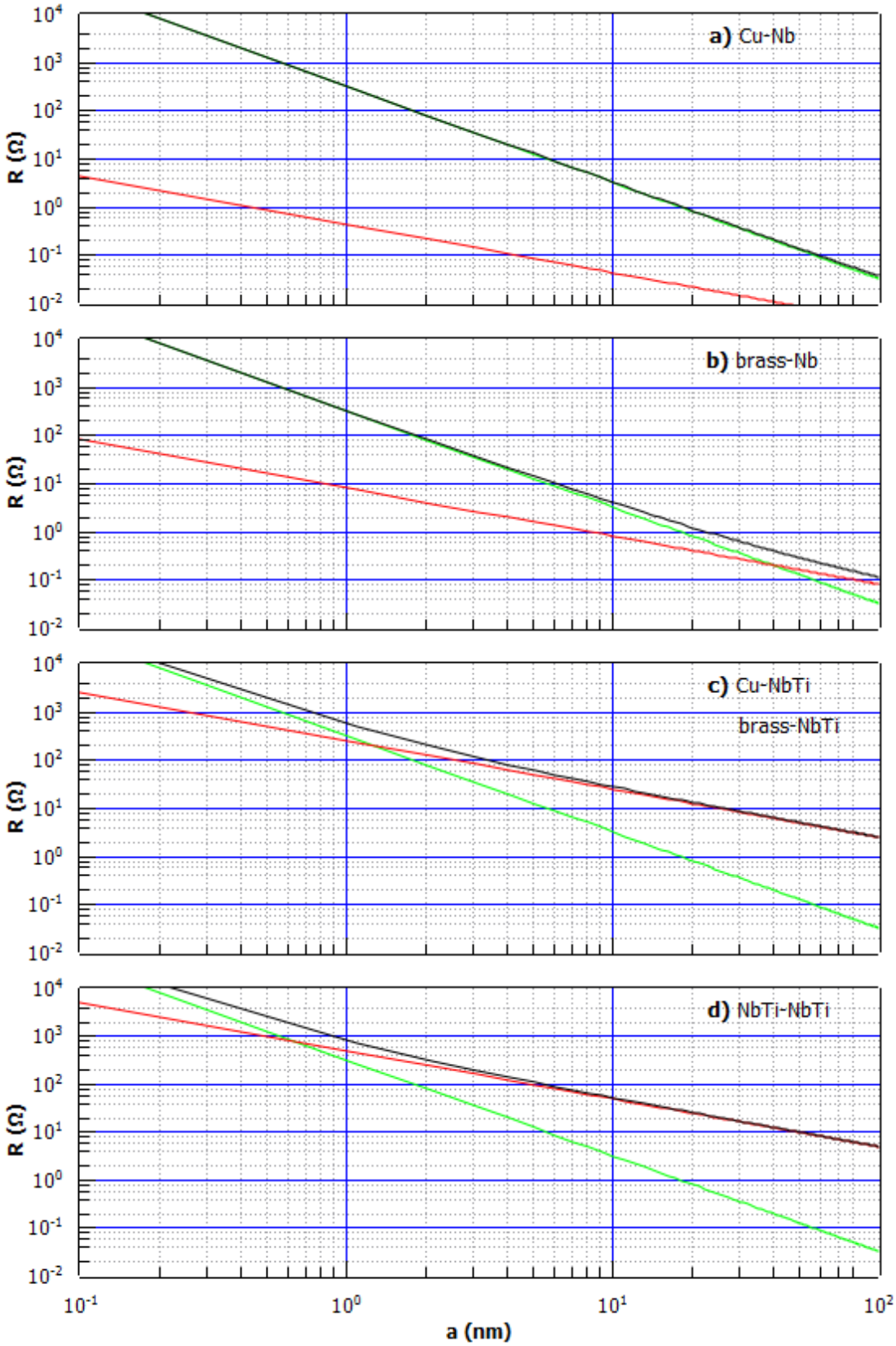

Figure 4. The Sharvin (green line), Maxwell (red line) and total (black line) resistances of the different pairings as functions of the contact radius.

3.3 Qualitative analysis of spectra

Before making any quantitative analysis the contacts were divided into three different categories based on their appearances. Firstly there were contacts with a double minimum, at least superficially similar to the expected AR spectra of an N-S contact. These were found in all pairings except the NbTi-NbTi (S-S) contacts. In all of them, the resistance dropped by a factor of less than two, meaning that AR could be an explanation for them. Secondly there were contacts with a single minimum. These were found in all the pairings. In those contacts the resistances usually dropped by a factor less than two, but there were some with a larger drop in the resistance, particularly in the S-S contacts. Thirdly there were contacts with a structure resembling the Josephson effect. They had a sharp (often discontinuous) transition in the differential resistance and a drop by a factor of more than two in the resistance at zero bias (for the S-S contacts the resistance usually dropped to zero). These were found in all pairings, but only at resistances below about 10 Ohms.

There was also a large number (roughly one half of the total) of contacts that did not fit into any of the above categories. Such contacts were left out of any further analysis. Nearly all of the spectra had some additional structure or background, but as long as the spectra could be placed in one of the above categories, such features were ignored when making the qualitative analysis. It should be noted that the above analysis is based solely on the appearance of the spectra. Figures (5)-(9) give examples of the various types of spectra, together with their I-V curves, for the different pairings.

Two things can be seen from the spectra: firstly nearly all of them have some kind of side peaks and secondly the contacts with NbTi did not contain a contribution from the normal state resistivity of NbTi. Based on the estimation in the previous section, the resistance of the NbTi contacts should come mostly from the Maxwell term. This means one would expect to see a large (close to one order of magnitude) rise in the resistance as one moves from the low-bias (superconducting) to the high-bias (normal). The only contacts that showed such behavior were the ”Josephson like” contacts, but as was mentioned above they were only present at resistances around 10 Ohms and further more such a spectrum (albeit only one each) were observed with the Cu-Nb and the brass-Nb contacts.

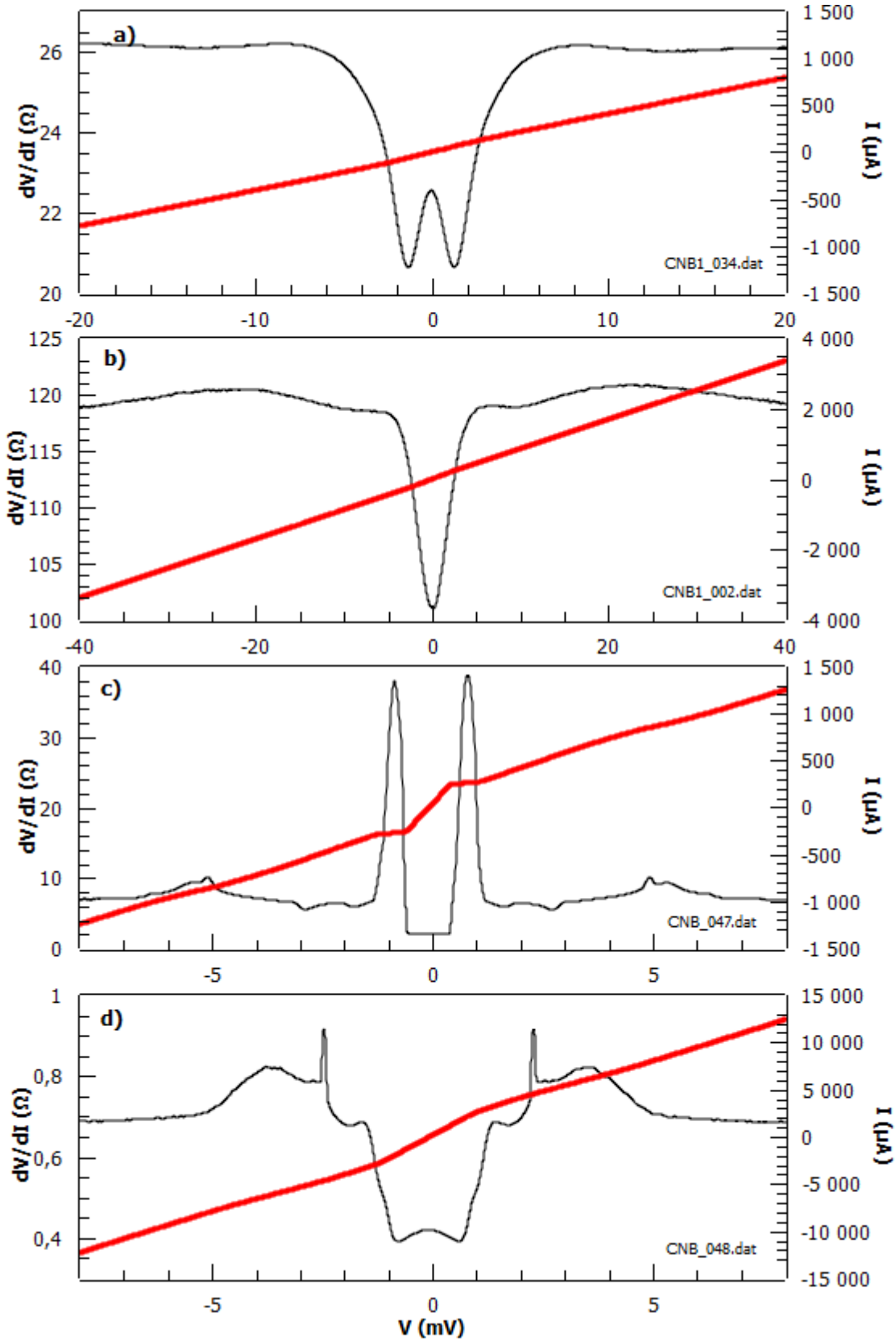

Figure 5. Typical examples of the different kinds of spectra of Cu-Nb contacts: a) a contact with a double minimum, b) a contact with a single minimum, c) a contact with a sharp transition and d) a contact that does not fit into any of the other categories.

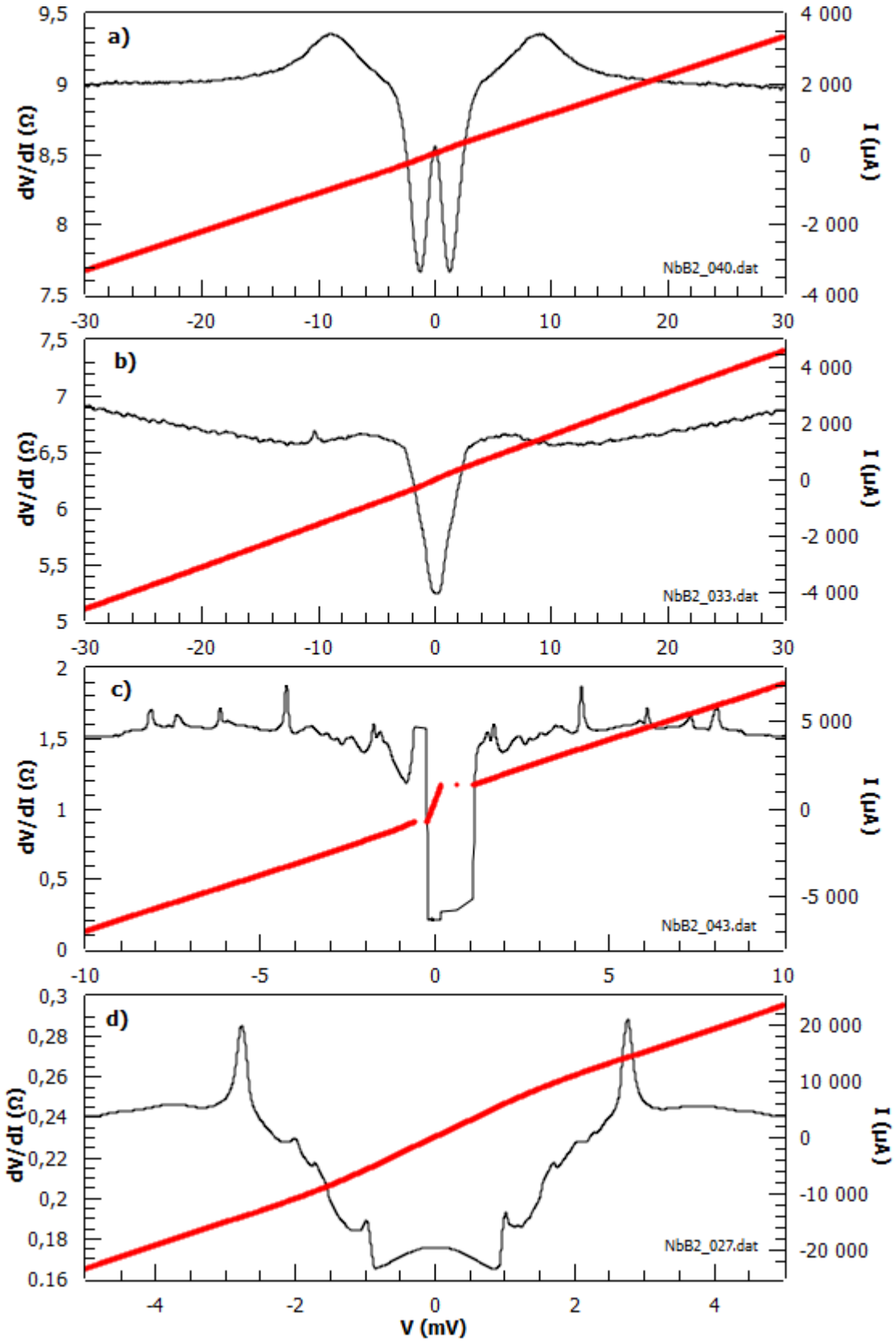

Figure 6. Typical examples of the different kinds of spectra of brass-Nb contacts: a) a contact with a double minimum, b) a contact with a single minimum, c) a contact with a sharp transition and d) a contact that does not fit into any of the other categories.

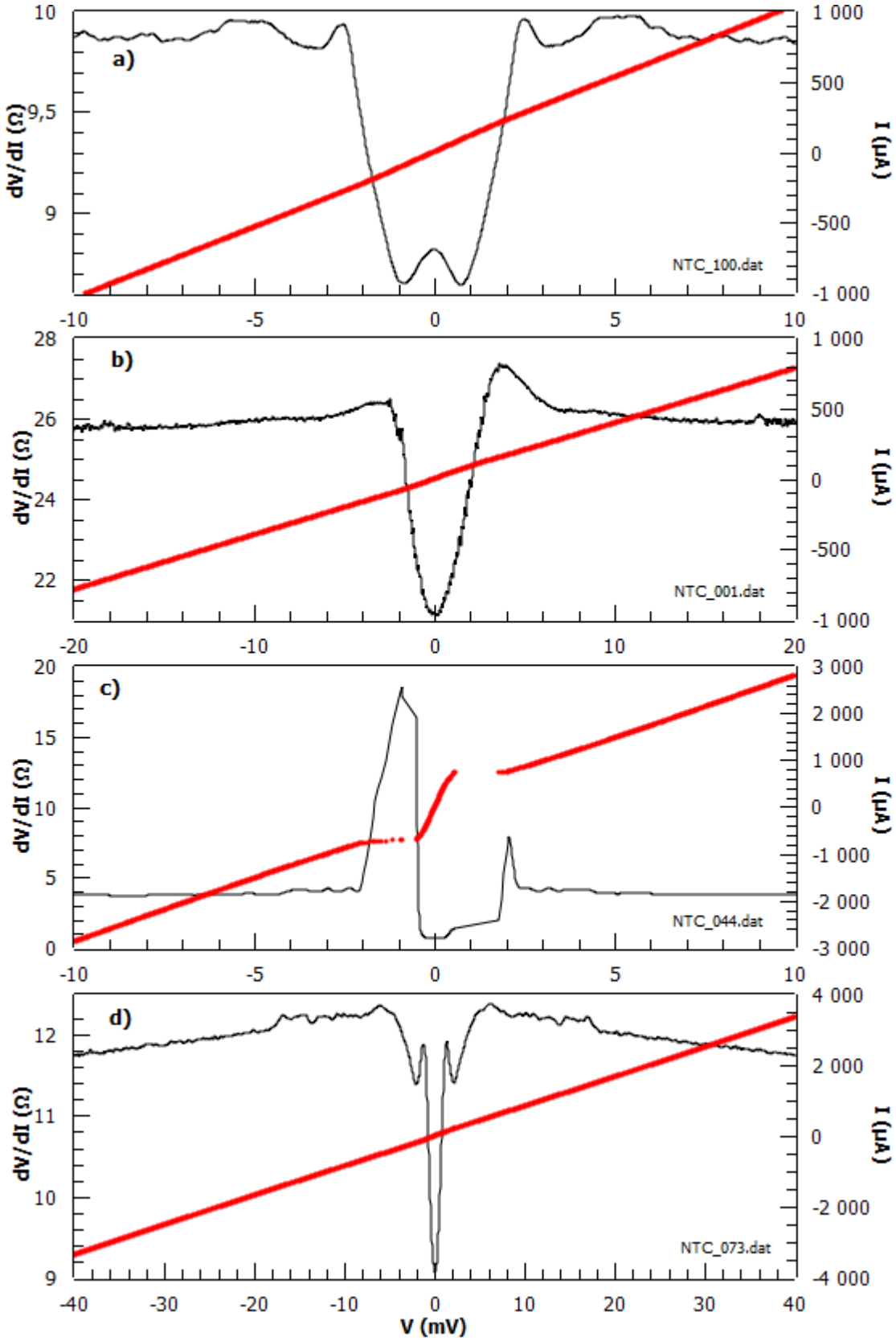

Figure 7. Typical examples of the different kinds of spectra of Cu-NbTi contacts: a) a contact with a double minimum, b) a contact with a single minimum, c) a contact with a sharp transition and d) a contact that does not fit into any of the other categories.

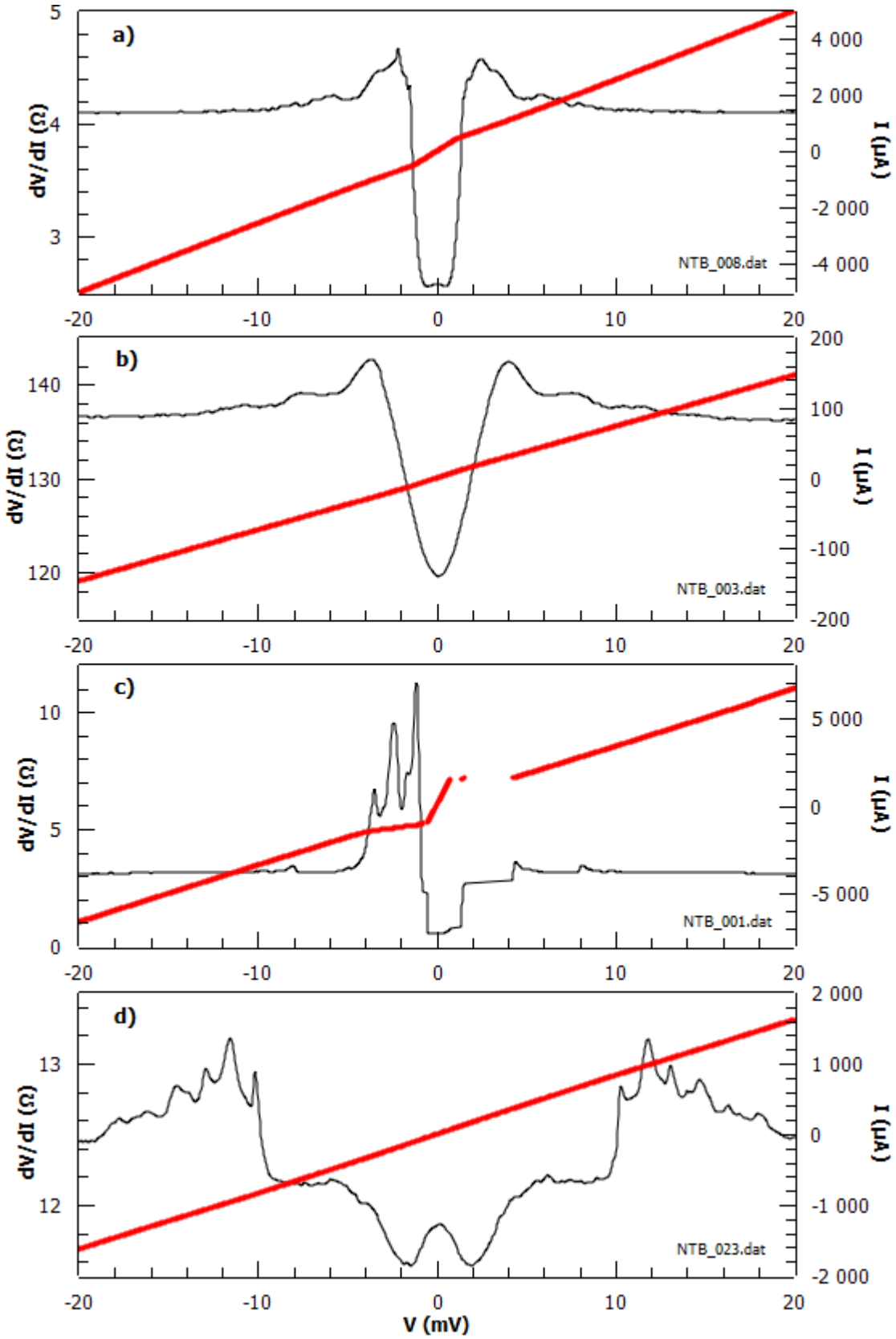

Figure 8. Typical examples of the different kinds of spectra of brass-NbTi contacts: a) a contact with a double minimum, b) a contact with a single minimum, c) a contact with a sharp transition and d) a contact that does not fit into any of the other categories.

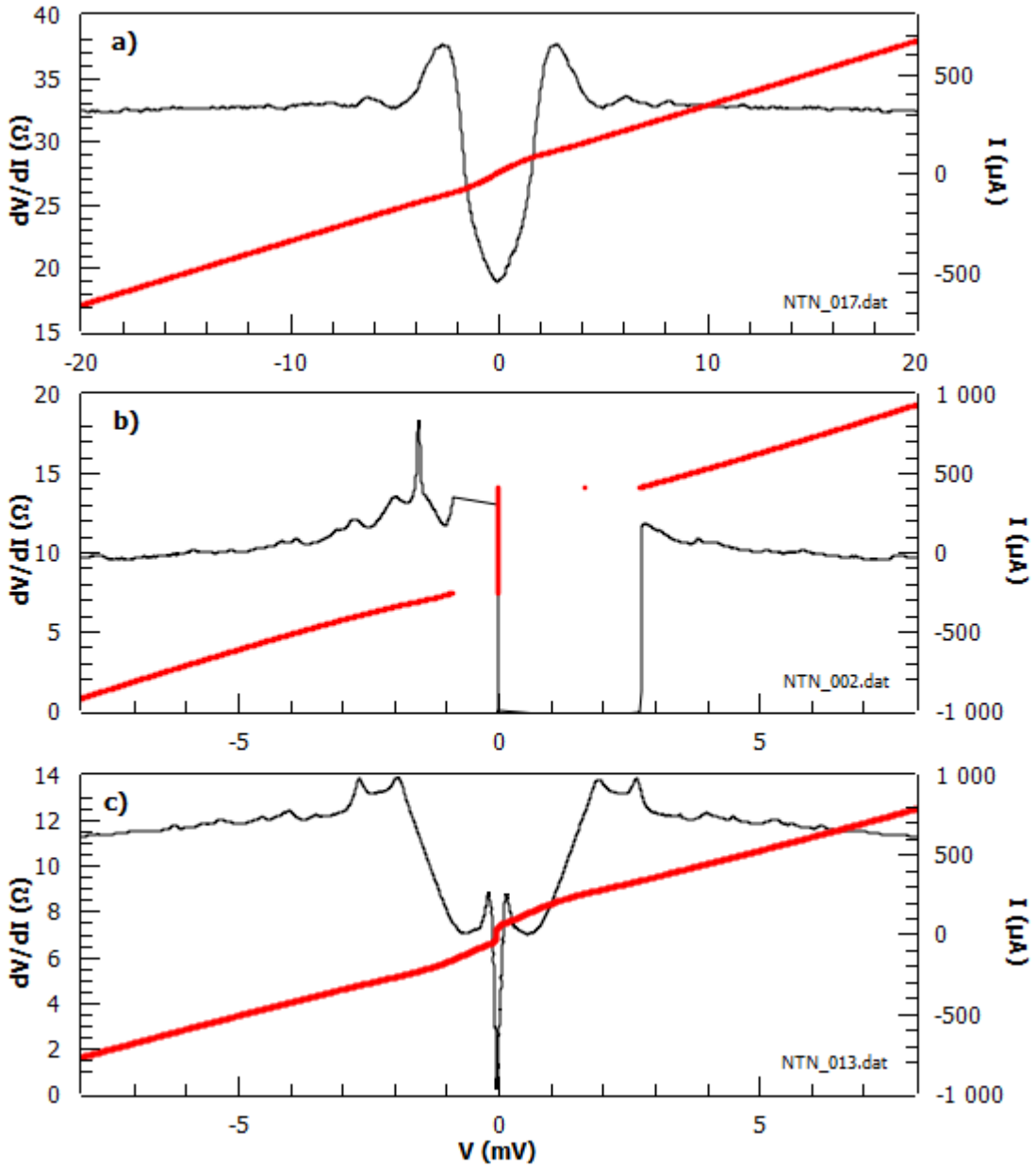

Figure 9. Typical examples of the different kinds of spectra of Nbti-NbTi contacts: a) a contact with a single minimum, b) a contact with a sharp transition and c) a contact that does not fit into any of the other categories.

3.4 Side peaks

The shape of the side peaks mentioned previously varied from broad ”shoulders” (fig. (6b)) to sharp peaks (fig. (5c)). Many of the contacts had multiple peaks. One way to explain the side peaks is to attribute them to the current reaching some critical value, where the superconductivity is weakened or destroyed in parts of the contact. In section 1.3 two mechanisms for such a critical current are given: the self-magnetic field and the pair-breaking current density.

To investigate whether one of them could be used to explain the side peaks, the critical currents are plotted as a function of contact resistance and contact radius in figures (10) and (11). The critical current was defined as the current at the maximum value of the side peak, for contacts that had multiple peaks the first (lowest current) significant one was used (what constitutes significant was in some cases somewhat arbitrary). In the "Josephson-like" spectra there were often no actual side peaks (fig. (9b) for example). In such cases the current, at which the transition occurred, was used. If a spectrum was asymmetric, the average of the critical currents was used. For the resistance the asymptotic value at high bias-voltage was used, or when no asymptote was present (fig. 6b) the value immediately outside the peak was used. To get the radii from the resistances, the relations plotted in figure (4) were applied.

If the peaks are caused by the self-magnetic field, the critical current should grow linearly with the radius (eq.(8)). If the peaks are caused by the pair-breaking current density, the critical current should grow as a square of the radius (eq.(9)). Based on figure (11) the self-magnetic field would seem as likely explanation for the NbTi contacts. The slope of the line around which the data points fall is close to one on the log-log scale indicating a linear dependence on the radius. For the contacts with Nb, a line with a slope of two can be drawn through the data points (albeit somewhat less convincingly than the line for the NbTi contacts). This corresponds to a quadratic dependence on the radius and would suggest that the pair-breaking current is the cause for the contacts with Nb. Looking at figure (11) and seeing as how the critical currents of the contacts with NbTi are smaller than the those of the contacts with Nb, it stands to reason that vortex formation, caused by the smaller lower critical field of NbTi, disrupts the superconductivity in the NbTi contacts before the pair-breaking current density becomes an issue.

Another way to interpret the results is to assume that the NbTi contacts are actually ballistic and that the conversion from resistance to radius in fig. (11) has not worked correctly. This way all the data points fall on the same line (fig. (10)) with a slope of -1, indicating a quadratic dependence on the radius, as the contacts are assumed to be ballistic. The quadratic dependence would suggest that the pair-breaking current density is the cause of the side peaks for both cases. If one assumes that NbTi has the same thermodynamic critical field and London penetration depth as Nb, then the fact that the data points for both Nb and NbTi fall on the same line (as opposed to when plotted as

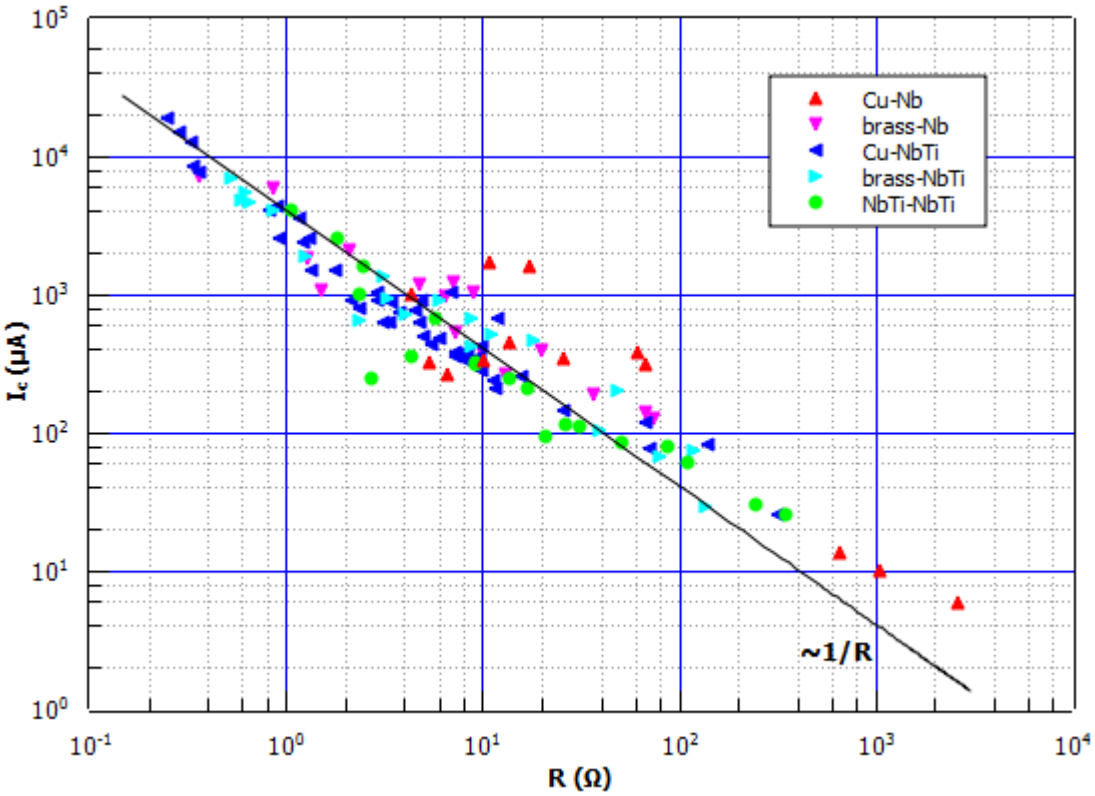

Figure 10. Critical currents of the different pairings as function of the contact resistance.

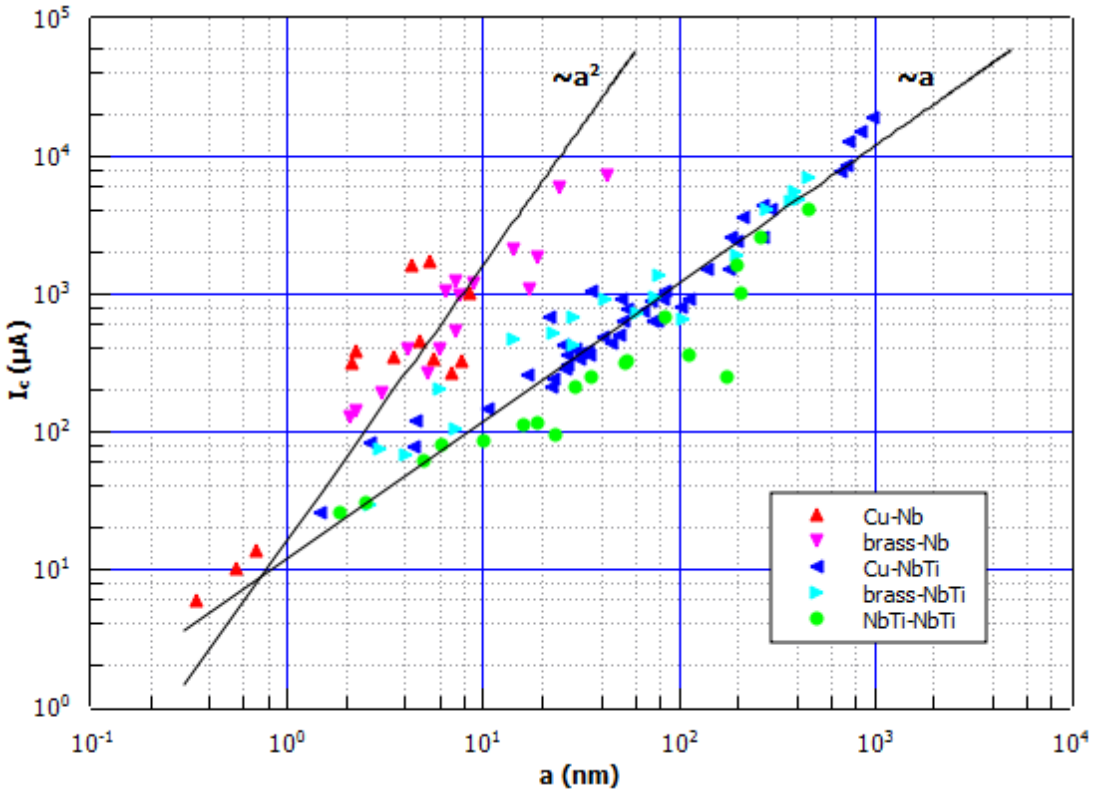

Figure 11. Critical currents of the different pairings as function of the contact radius.

function of radius), lends some credibility to this interpretation, as the critical current from the pair-breaking current density depend on the thermodynamic critical field and London penetration depth. But in the end this reasoning still depends on the questionable assumption, that the NbTi contacts are ballistic. With this in mind it would seem more likely, that the fact that all the data points fall on the same line is merely a coincidence.

Similarly it could be argued that the pure metal contacts are not ballistic, but in the thermal or diffusive limit. This could be explained by the distortion of the crystal lattice near the contact. In this way the slope of -1 would indicate a linear dependence on the radius, as the contacts are all assumed to be non-ballistic. The linear dependence would imply that the self-magnetic field is the cause of the side peaks. The problem with this, is that both the upper and lower critical fields of Nb and NbTi are very different. The data points should not fall on the same line.

To estimate the critical currents one would expect for the Nb contacts from the self-magnetic field and the pair-breaking current, the literaure value of 0.2 T [15, p729] is used for the thermodynamic critical field. As the values for the upper and lower critical fields of Nb can vary depending on the sample and the values for the samples used in this study were not measured, the same value of 0.2 T is used for the case of the self-magnetic field. For the London penetration (λ_L) depth 40 nm is used [17]. Inserting these values into eq. (7) and (8) one gets for a contact with a radius of 10 nm the following critical currents. For the self-magnetic field

$$I_c = \frac{2\pi a B_c}{\mu_0} = \frac{2\pi \cdot 10\,\mathrm{nm} \cdot 0.2\,\mathrm{T}}{1.256\,\mu\,\mathrm{N/A^2}} = 10\,\mathrm{mA} \quad ,$$

and for the pair-breaking current

$$I_c = \frac{4 B_{c,th}}{3\sqrt{6}\,\mu_0 \lambda_L} \cdot \pi a^2 = \frac{4 \cdot 0.2\,\mathrm{T}}{3\sqrt{6} \cdot 1.256\,\mu\,\mathrm{N/A^2} \cdot 40\,\mathrm{nm}} \cdot \pi (10\,\mathrm{nm})^2 = 0.680\,\mathrm{mA}$$

The value given by the pair-breaking current is off only by a factor of two, a good match with the line connecting the data points for the Nb contacts. This would mean that the pair-breaking current is the likely cause of the side peaks for the Nb contacts.

For the NbTi we assume that the London penetration depth and the thermodynamic critical field are the same as those of Nb. The upper critical field is, as was mentioned previously, approximately 12 T. Using eq.(7) the lower critical field can be estimated to

be roughly 0.0033 T. As above inserting these values into eq. (8) and (9) one gets the following critical currents for a contact with a radius of 10 nm. For the self-magnetic field with the upper critical field

$$I_c = \frac{2\pi a B_c}{\mu_0} = \frac{2\pi \cdot 10\,\mathrm{nm} \cdot 12\,\mathrm{T}}{1.256\,\mu\,\mathrm{N/A^2}} = 600\,\mathrm{mA}$$

and for the self-magnetic field with the lower critical field

$$I_c = \frac{2\pi a B_c}{\mu_0} = \frac{2\pi \cdot 10\,\mathrm{nm} \cdot 0.0033\,\mathrm{T}}{1.256\,\mu\,\mathrm{N/A^2}} = 0.165\,\mathrm{mA} \quad ,$$

for the pair-breaking current the critical current is the same as with the Nb contacts. The critical current derived from the upper critical field is far too big, but the one from the lower critical field is almost a perfect match with the line connecting the NbTi data points. Since the lower critical field was used, this would mean that the process of vortex formation is sufficient to destroy or disrupt the superconductivity in the contact region.

The absolute values of the critical currents for both the Nb and NbTi contacts are in agreement with the interpretation that the side peaks of Nb and NbTi are caused by different mechanisms, the pair-breaking current for the Nb contacts and the self-magnetic-field for the NbTi contacts.

Our assumption that NbTi has the same London penetration depth as Nb, may well be inaccurate. Literature sources give a value of 300 nm [18, p576]. This would mean that for a NbTi contact with a radius of 10 nm, the critical current caused by the pair-breaking current would be slightly smaller than the one caused by the self-magnetic field. This in turn would mean that the slope of the line connecting the NbTi data points should change to two when the contacts are small, as the pair-breaking current density is reached before the critical magnetic field. But the fact that no such change can be seen is not too worrying, as the above calculations are intended to be just rough estimates.

There is also the possibility, that the side peaks are caused by local-heating. If this is the case, then the voltages of the side peaks should correspond to local temperatures of about 10 K, the critical temperature of both superconductors. Using eq. (4) one can estimate, that at a bath temperature of 4 K, this would mean voltages of around 2.5 mV. The voltages corresponding to the peaks are given in figure (12).

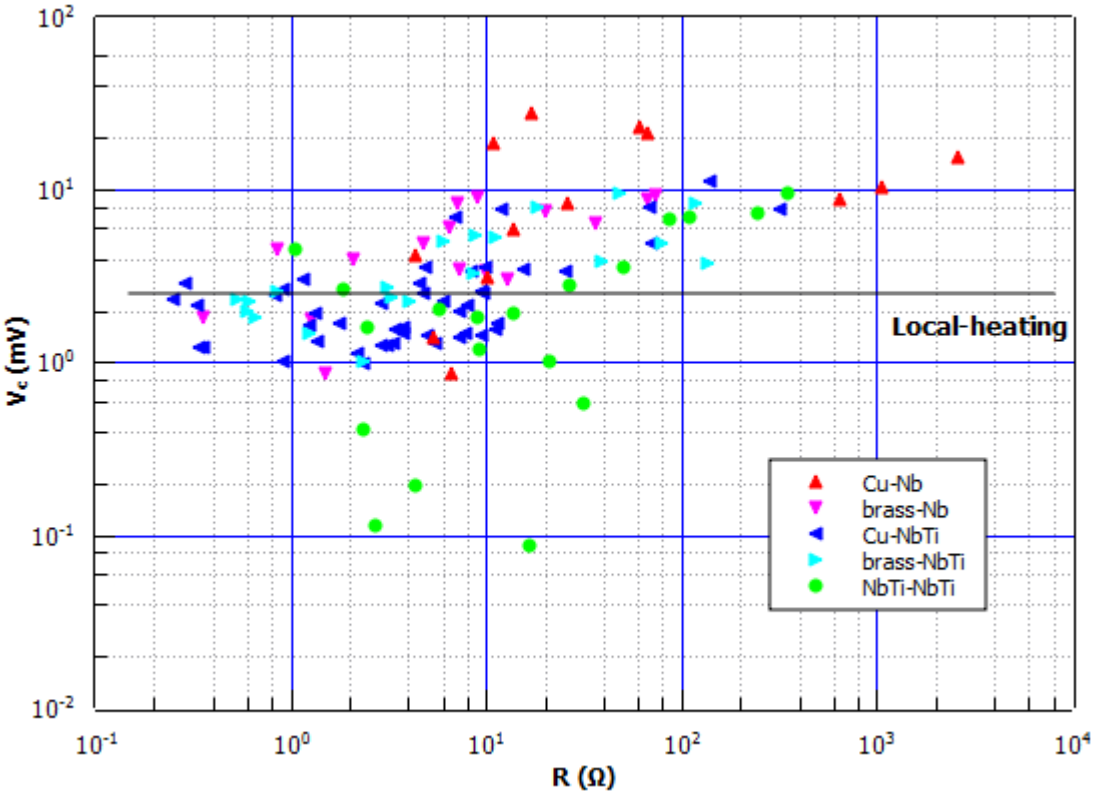

Figure 12. Critical voltages of the different pairings as a function of resistance.

While at first glance the voltages seem to be near the expected 2.5 mV there are two major problems. Firstly, for a number of the NbTi-NbTi (S-S) contacts the voltages are so low that local-heating plays no part and also for a good number of the other contacts the voltages are so low, that local-heating cannot be the only explanation. Secondly the Cu-Nb and brass-Nb contacts are ballistic, so there should be no local heating for those contacts and yet they still have the sidepeaks. If there is local-heating, then it should be observed in the NbTi-NbTi contacts and not in the Cu-Nb and brass-Nb contacts. Considering these two things it seems unlikely, that local-heating would be the cause of the side peaks. The slowly rising value of the critical voltage seen in figure (12), is probably just due to the approximately 1/R-dependence of the critical currents seen in figure (10).

The temperature dependence of the side peaks was also studied. For a number of contacts the spectra were measured at temperatures ranging from 1 K to 10 K. Figure (13) shows one such temperature series for a brass-NbTi contact. As with the constant temperature measurements, only the spectra that fell into one of the three categories mentioned in section 3.3 were analyzed. This resulted in a total of eight temperature series: two with Cu-NbTi, three with brass-Nb and three with brass-NbTi. There are no

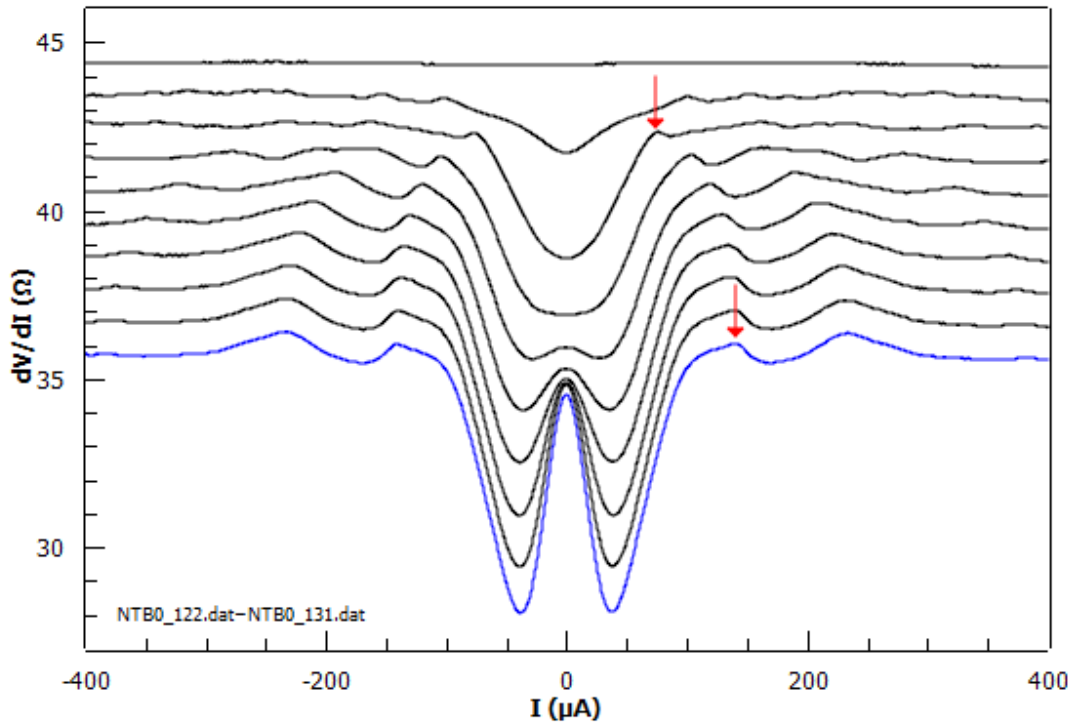

Figure 13. A temperature series for a brass-NbTi contact. The lines are offset by 1 Ohm for every 1 Kelvin from the value at 1K (blue line). The arrows indicate the side peaks at 1K and at 8 K.

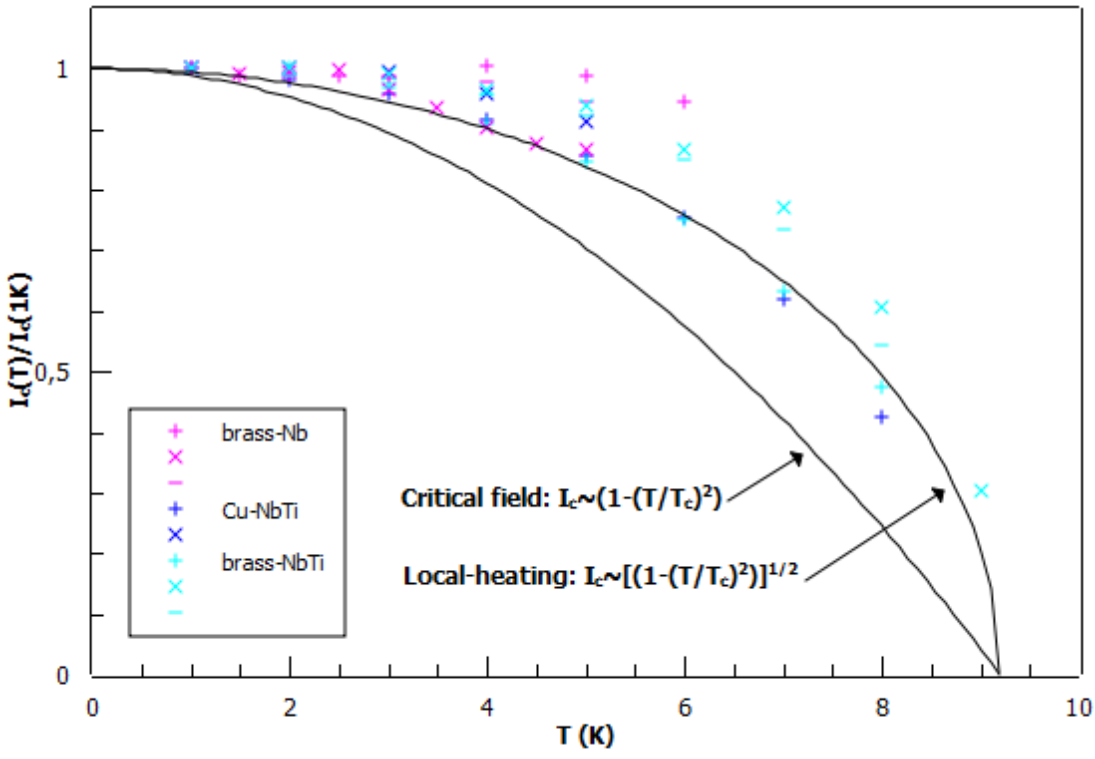

Figure 14. The critical currents as a fraction of the critical current at 1 K, for a number of contacts. The solid curves correspond to the temperature dependence from the critical magnetic field $I_c \sim (1-(T/T_c)^2)$ and a temperature dependence from local-heating $I_c \sim [(1-(T/T_c)^2)]^{1/2}$, with a T_c of 9.2 K.

temperature series for Cu-Nb, because the Cu-Nb data came from earlier measurements, that were all carried out at 4.2 K. The critical currents at different temperatures are plotted in figure (14) as a fraction of the critical current at 1 K.

For almost all of the contacts the peaks became indistinguishable before reaching the critical temperature. This together with the relatively large differences between the different contacts seen in fig. (14) makes it difficult to draw any conclusions from the temperature dependence. All that can be said is that the shape of the curves are closer to a $((1-(T/T_c)^2))^{1/2}$ dependence resulting from local heating, than to a $(1-(T/T_c)^2)$ dependence resulting from the temperature dependence of the critical magnetic field (both with a critical temperature of 9.2 K). This would be in agreement with the local-heating model (the T in eq. (4) becomes T_c, T_{bath} becomes T and U is proportional to I). This interpretation for the cause of the side peaks would contradict the interpretation based on the size and voltage dependencies mentioned above.

3.5 Josephson-like contacts

The ”Josephson-like” contacts look very different from the other contacts, but their critical currents fall on the same line with the other contacts in fig. (10). This would suggest that the mechanism behind the sharp transition in the ”Josephson-like” contacts and the side peaks in the other contacts is the same. The ”Josephson-like” spectra varied from the relatively smooth transitions such as that in fig. (5c) to the sharp and discontinuous transition in fig. (9b). Some of the spectra had such a sharp transition that the lock-in amplifier could not keep up with it, resulting in strange looking differential resistance spectra.

The biggest difference between the ”Josephson-like” and the other contacts is that in the former the resistance always drops by a factor larger than two. There were some contacts in the single minimum category, where the resistance also dropped by more than a factor of two, but they were less common. This means that the drop in the resistance at zero bias cannot be explained with Andreev reflection. As was mentioned previously one explanation would be to attribute the drop in the resistance to the vanishing Maxwell resistance of the NbTi. However, this does not explain why such spectra were also seen with the Nb contacts. Unless one is willing to ignore the ”Josephson-like” spectra of the Nb contacts as anomalies or assume that the normal

state resistivity of Nb has increased many fold (for example due to lattice distortions caused by the pressure applied to the contact), the vanishing Maxwell resistance cannot be a satisfactory explanation. Another explanation would be to assume that the NbTi or Nb induces superconductivity into the normal electrode through the proximity effect. In this way the contact would behave like a Josephson junction, allowing the resistance to drop by more than the factor of two of Andreev reflection, without the need for a high normal state resistivity.

Another thing worth noting is that the ”Josephson-like” spectra were only found in contacts with small normal resistances. Since smaller resistances correspond to larger contacts, this agrees with the vanishing Maxwell resistance explanation: As one reduces the resistances of the contacts to around 10 Ohms the Maxwell term begins to dominate and the contacts would become diffusive or thermal. Another explanation would be that the large contact sizes allow the proximity effect to take place.

Some, but not all, of the ”Josephson-like” contacts had a kind of hysteresis. When approaching the transition from the high bias (non-superconducting) side the critical currents were lower than when approached from the low-bias (superconducting) side. Figure (15) shows the I-V curves of a contact with such a hysteresis. It contains two measurements of the same contact: one is done from negative to positive bias and the other from positive to negative. It would appear that the presence of the superconductivity resists the transition to the normal state. This could be due smaller heat dissipation in the contact, when it is in the superconducting state.

The variance of the voltage was measured for a transition in one of the “Josephson-like” NbTi-NbTi contacts. The measurement system takes several hundred voltage measurements for every value of the current and the average of those is taken as the value of the voltage for that particular current. The individual voltage measurements are not stored as they are usually of little interest and storing them would result in very large files. What is stored is the variance of those individual measurements. This variance can be considered as electrical noise. Figure (16) shows the I-V curve and the noise of the transition for one such contact.

Looking only at the I-V curve, it would seem like the transition is continuous, if a bit unstable, the voltage getting all the intermediate values as the current is being swept.

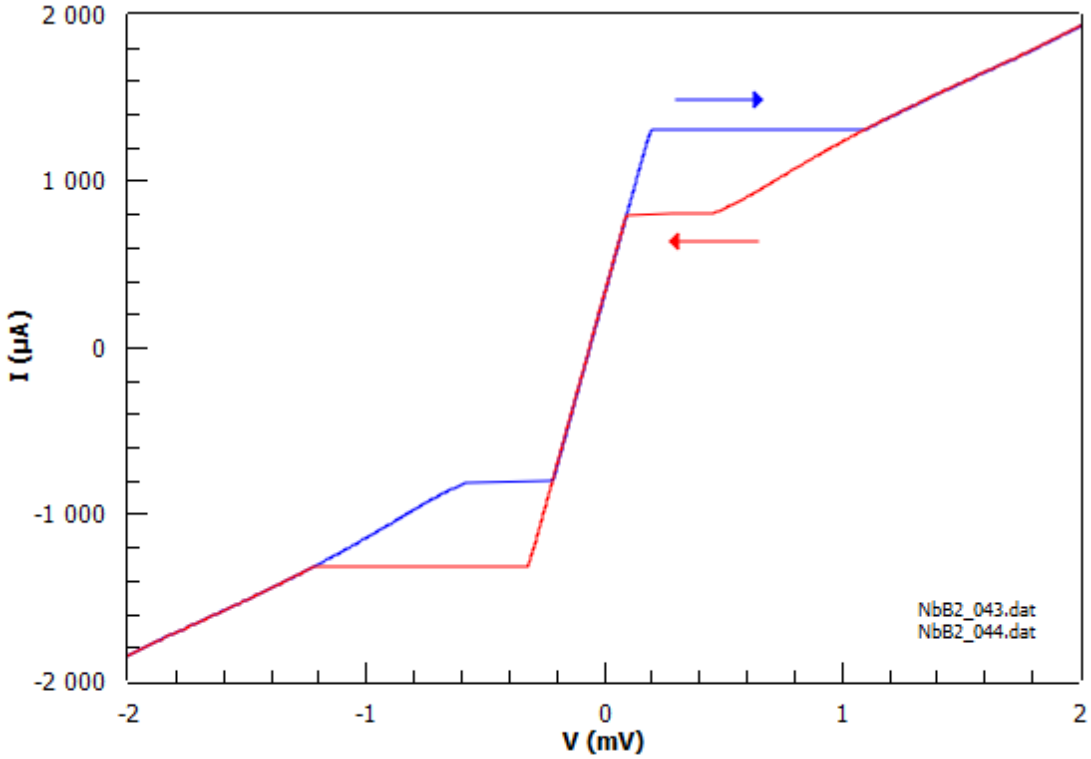

Figure 15. A contact with hysteresis. The contact is the same for both of the measurements, but the sweeps are done in opposite directions. The value of the critical current depends on which side the transition is being approached from.

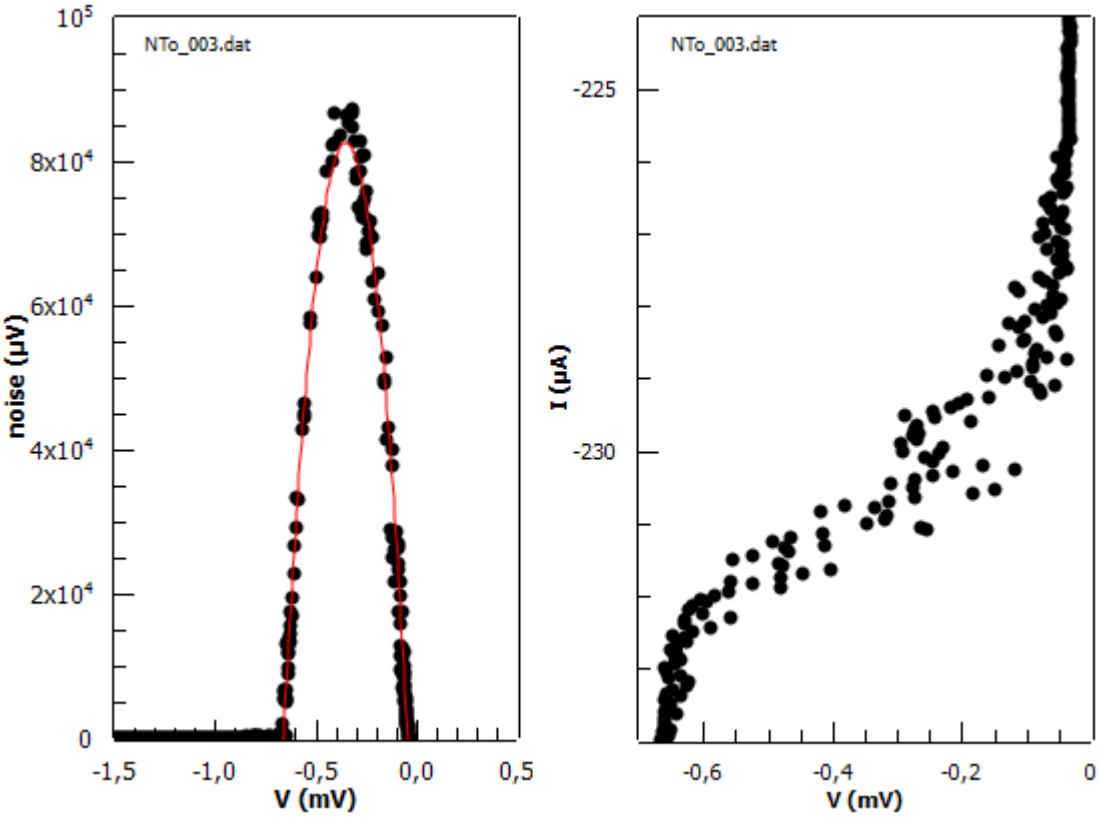

Figure 16. A transition in a "Josephson-like" NbTi-NbTi contact. On the left: The noise of the transition. The red line is a square fit to the data. On the right: The I-V curve of the transition.

But it is probably more likely, that the voltage is jumping between the two sides of the transition in a discontinuous manner and the continuity of the I-V curve is just due to the measurement system averaging the voltage values. If this is the case then the variance of the transition should have the shape of

$$\Delta V^2 \sim (1-x)\cdot x^2 + x\cdot(1-x)^2 \quad ,$$

where x is a number between 0 and 1 giving the position on the transition. The linear terms give the probabilities of an individual measurement being either on the left or the right side of the transition. The quadratic terms are the squares of the distances from the recorded average voltage, that is the variance from that individual measurement. The variance of the complete measurement (at a certain voltage) is then the average of variances of the individual measurements. The shape is a parabola with the maximum at the center of the transition. At the maximum the variance should reach a value that is equal to one quarter of the square of the width of the transition. For the transition in figure (16) this would mean roughly 100 000 $(\mu V)^2$, a value that is quite close to what was actually measured.

This hypothesis would have been easy to check if the individual voltage measurements had been saved, but since they were not, all that can be said is that the shape and the size of the noise spectrum agrees with the interpretation that the contact is switching between the normal and the superconducting sides during the transition. It should be noted that this particular explanation for the shape and magnitude of the noise spectrum depends on the frequency at which the contact switches between the superconducting and normal states being low enough, so that the measurement system can keep up with the process.

3.6 Sizes of the superconducting minima

The amount by which the resistances of the contacts were reduced by the superconductivity varied from the completely disappearing resistances of some of the S-S contacts to a reduction of just a few percentages for some of the high resistance contacts. To see whether there is some kind of systematic behavior in the sizes of the superconducting minima the relative drops in the resistance (the difference between the normal-state resistance and the minimum resistance divided by the normal-state resistance) are plotted as a function of the contact resistances in figure (17).

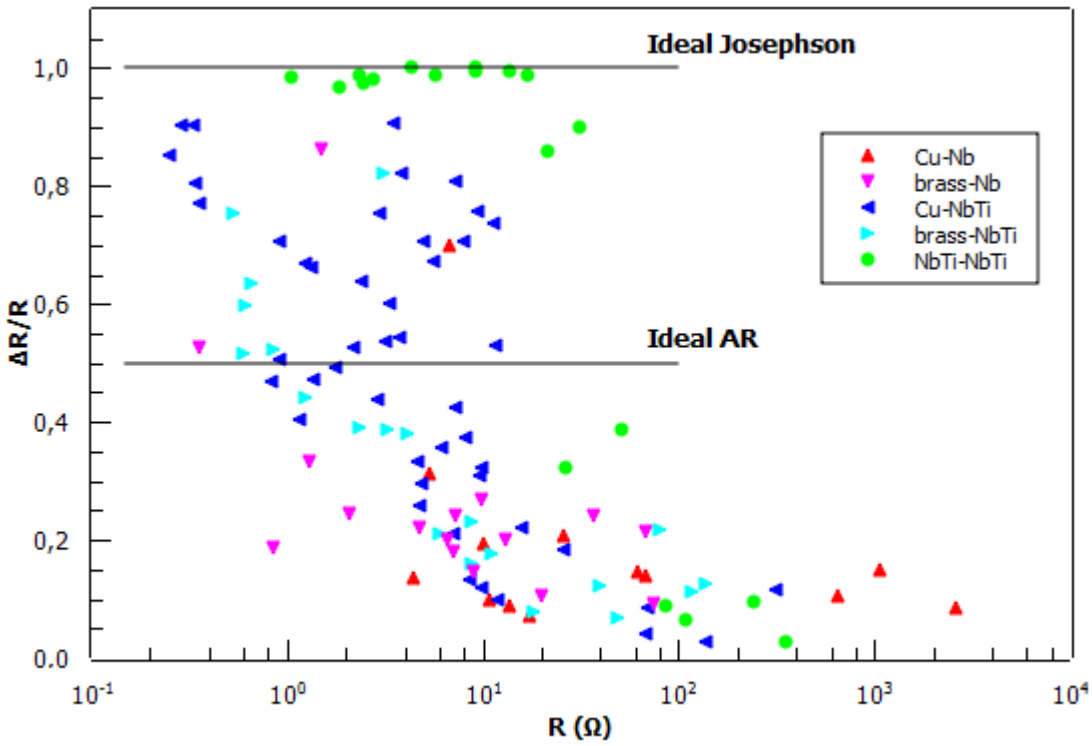

Figure 17. The relative drops in the resistances as functions of the contact resistance.

The spectra where the resistance drops by more than a factor of two are only present at the lower resistances and there is a slight trend towards smaller superconducting effects at higher resistances. Otherwise there is really no systematic in the way the sizes of the superconducting effects vary. The NbTi-NbTi contacts near the "Ideal Josephson" line can be explained by the Josephson effect, possibly combined with a contribution from the Maxwell resistance. Similarly the N-S contacts below the "Ideal AR" line can be explained by Andreev reflection. The contacts between the two lines are a more difficult matter. They certainly cannot be explained by AR, which leaves either the Josephson effect, the vanishing Maxwell resistance or a combination of the two as the possible explanations. This is discussed further in section 4.3.

3.7 BTK-fits

Many of the contacts had a double minimum structure that resembled what the BTK-theory predicts for a ballistic contact with Andreev reflection. Furthermore the double minimum structures were not present in the S-S contacts, suggesting that AR would be the cause of the double minima. To study whether AR really is the cause of the double minima, a number of spectra were fitted with the BTK-model modified to include the

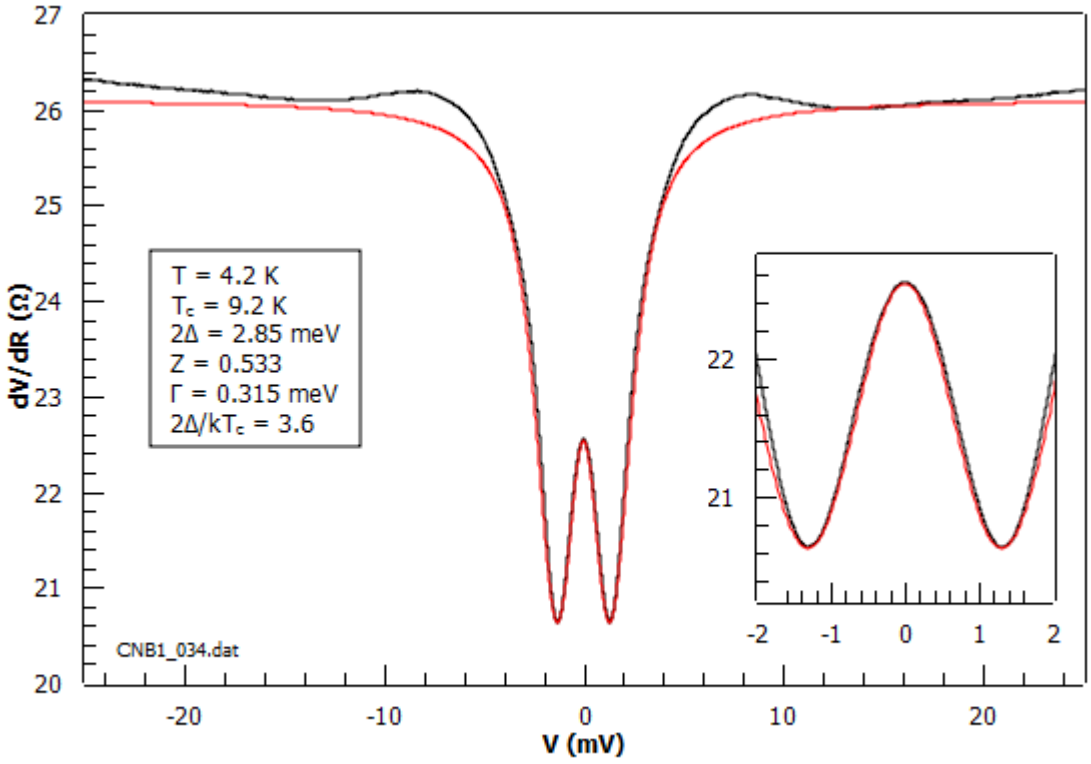

Figure 18. A spectrum for a Cu-Nb contact with a BTK-fit.

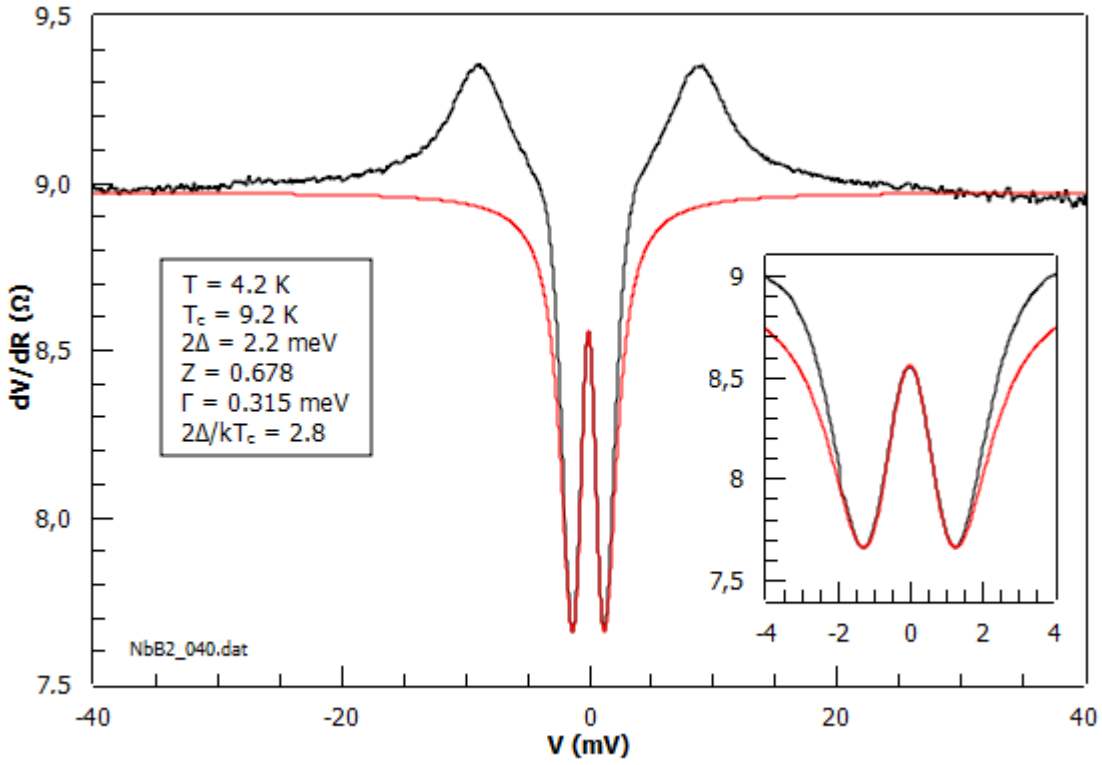

Figure 19. A spectrum for a brass-Nb contact with a BTK-fit.

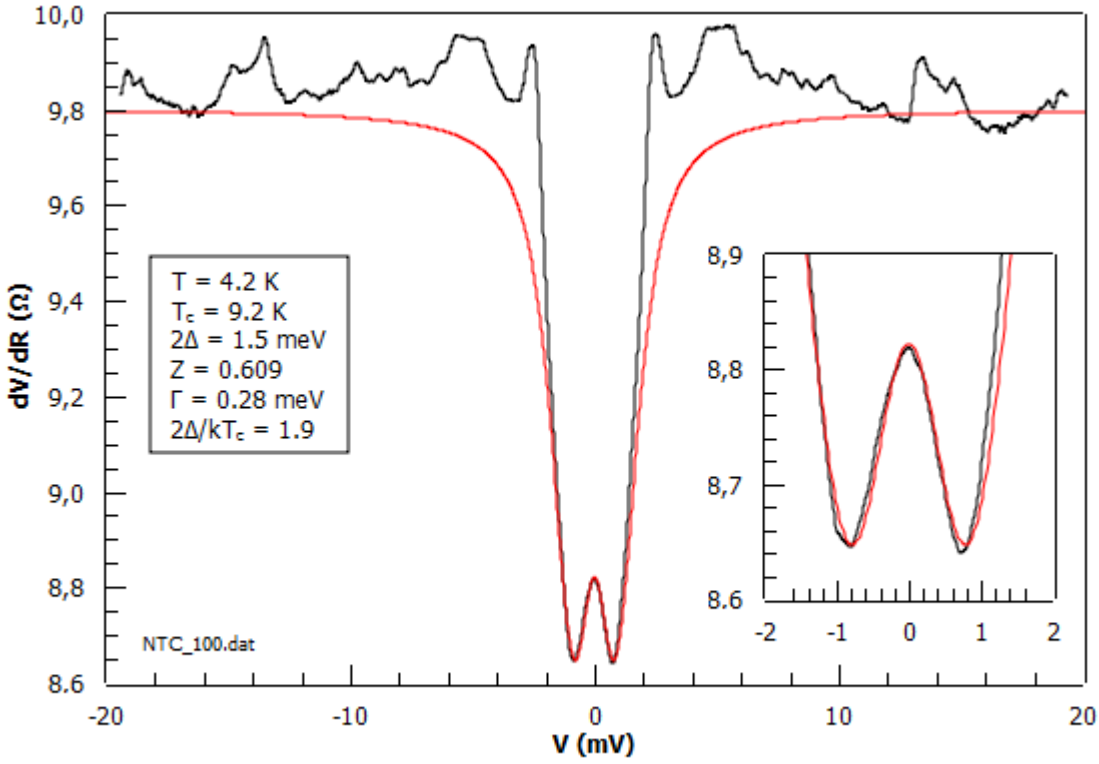

Figure 20. A spectrum for a Cu-NbTi contact with a BTK-fit.

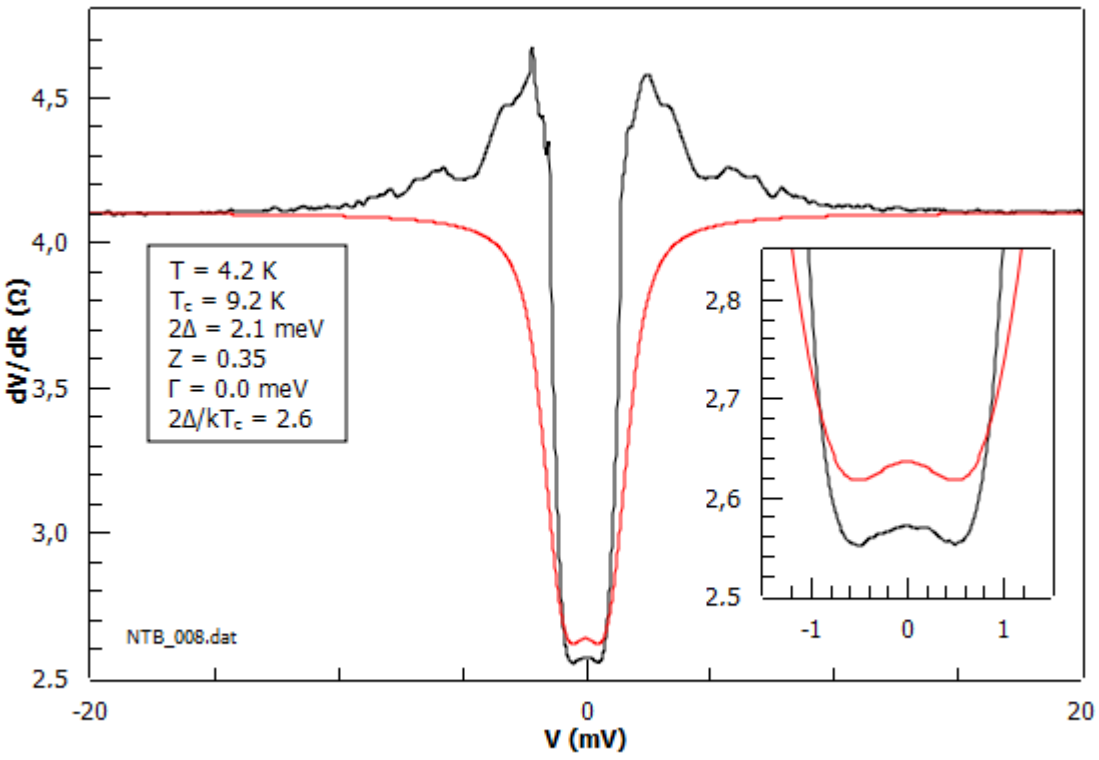

Figure 21. A spectrum for a brass-NbTi contact with a BTK-fit.

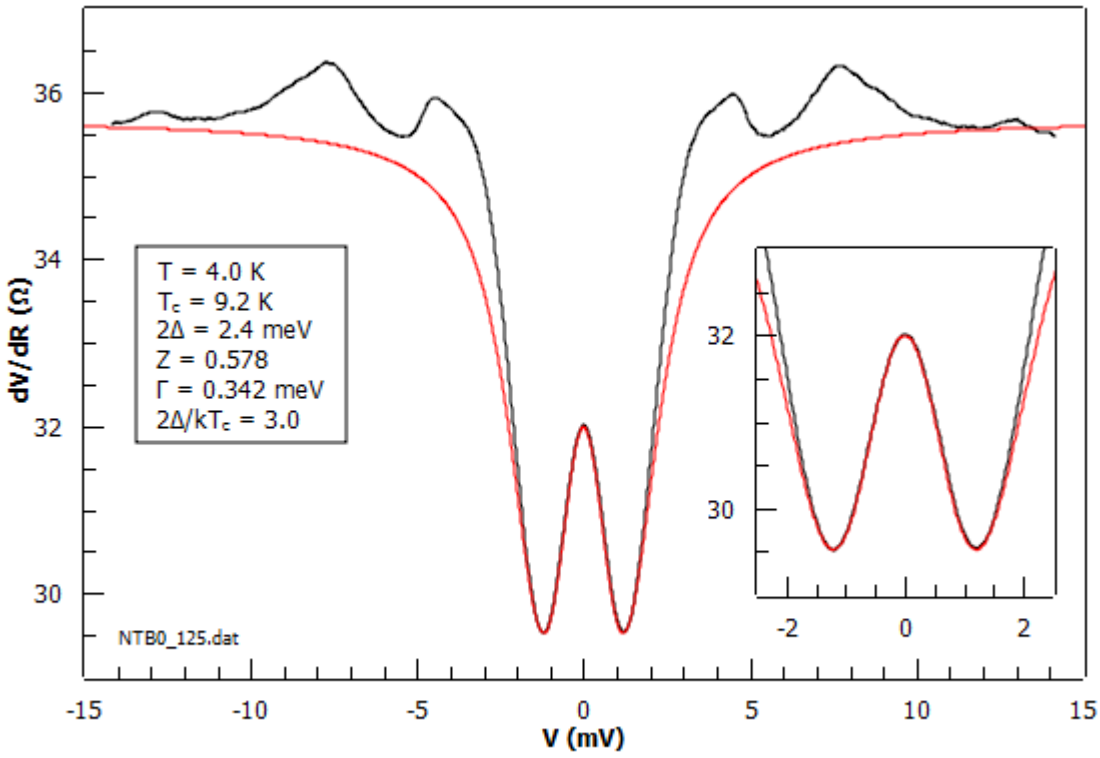

Figure 22. A spectrum for a brass-NbTi contact with a BTK-fit.

lifetime effect. The double minimum spectra in figures (5)-(8) and the NbTi-brass spectrum in figure (13) were used.

The fitting was done by manually adjusting the parameters until the fit coincided with the measured data. The fits and their parameters together with the measured data are given in figures (18)-(22). Apart from the side peaks and a small background, the fit to the Nb-Cu spectrum coincided nearly perfectly with the measured data. With the other contacts the shapes of the maxima at zero-bias and the depths of the minima were reproduced (except for one of the two brass-NbTi contacts), but the fit began to deviate from the measured data further away from the zero-bias.

There are a number of possible reasons why the fits differ from the measured data. The first would be that the double minimum features are not caused by AR at all (except for the Cu-Nb contact), but this seems unlikely considering how well the fits coincide near zero-bias. Another explanation would be that the effect from a diffusive layer at the contact is changing the shape of the spectrum. Thirdly the difference may be caused by side peaks. If the side peaks begin to appear already at low bias-voltages, it is possible that the steeper rise of the resistance can be caused by the side peaks being superposed

on the features caused by the AR process. Finally it may be caused by a contribution from the normal state resistivity of the superconductor being superposed on the features of the AR process, but this should not be the case for the brass-Nb contact.

4. Discussion

4.1 Missing Maxwell contribution

The fact that the spectra for the NbTi contacts did not contain a well-defined contribution from the vanishing normal state resistivity of NbTi, is a major problem. Based on the estimates in section 3.2, the resistance of a NbTi contact should have been mostly caused by the high normal-state resistivity of NbTi, that vanishes below T_c. Therefore there should have been a large change in the resistance, as the voltage sweep went from high bias to low bias. The observed changes in the resistance were often much smaller than the estimated sizes of the Maxwell resistances. Only in the larger contacts, with normal-state resistances below about 10 Ω, did the resistance drop by a factor of more than two, suggesting that the higher resistance contacts could in fact be ballistic. Determining whether or not the contacts are ballistic is amongst the first things one should do when analyzing point contact measurements. Any ambiguity on answering that question will cast serious doubts on the rest of the analysis.

If the NbTi contacts are indeed ballistic, then the following question needs to be answered: What went wrong in the conversion from resistances to radii done in section 3.2? The first possible explanation is related to the parameters used in eq.(5), the Fermi wave number and the resistivity. The Fermi wave number that was used was an estimate, not an actual measurement. If the actual wave number was smaller, the contacts would become more ballistic as the Sharvin resistance of a contact is inversely proportional to the square of the Fermi wave number.

Similarly a lower resistivity would reduce the Maxwell resistance of a given contact, making it more ballistic. The fact that the bulk resistivity of the sample wire was actually measured separately, makes this explanation less likely. One could still argue that, since what was measured was the resistivity of the bulk, which is not necessarily relevant for the point contact, there may be some kind of surface effect that changes the resistivity. Such an effect would be more likely to increase the resistivity of the surface

region, as the increased pressure caused by the creation of the point contact distorts the lattice, creating defects. One way in which the resistivity could decrease would be, if a layer of pure Nb formed at the surface of the NbTi. If such a layer existed, it would probably be only a few atomic layers deep and therefore too small (the depth of the layer would need to be several nanometers, the sizes of the contacts). As such this explanation seems very unlikely.

Multiple contacts is another possible explanation. In this case the measured spectrum would be the combined result of several separate contacts. Having multiple contacts in parallel would mean that the resistances of the individual contacts would be higher than the measured total resistance. While this explanation could account for the missing Maxwell resistance, as it would make the contacts more ballistic, it does not come without problems. If there indeed are multiple contacts, then each individual contact should have its own *Z* parameter and quite possibly own energy gap as well. Because of this, one would expect the resulting spectra to be a good deal more complex, but instead the BTK-fits in section 3.7 coincide fairly well with the measured data.

Finally there is the possibility of a negative proximity effect, a non-superconducting layer of NbTi at the point contact. If the part of the NbTi that contributes to the Maxwell resistance is not superconducting, then the Maxwell resistance should remain constant during the measurement. Andreev reflection can still take place deeper inside the NbTi. The problem with this explanation is that the sizes of the superconducting effects should be much smaller as the constant Maxwell resistances dominate the contacts. For a 10 Ω NbTi contact the Sharvin resistance is only about 5 % of the total resistance (fig.(4)), but the sizes of the superconducting effects are considerably larger (fig.(17)).

Actually proving or disproving any of the above explanations would be quite difficult and would certainly fall outside the scope of this study. The idea of the smaller Fermi wave number seems the most straightforward. Because of the quadratic dependance in eq.(1), the error in the value of the wave number does not need to be as large as with the resistivity. Reducing the wave number to one tenth, would increase the Sharvin resistance hundredfold. Still, while this would be enough to make the contacts mostly ballistic throughout the measurement range, it is very unlikely that the Fermi wave number would be so low.

4.2 Causes of the side peaks

Based on how the critical currents depend on the contact radii (fig (11)) and on the actual values of the critical currents, it can be argued that the cause of the side peaks in the Nb contacts is due to the critical current density being exceeded and in the NbTi contacts due to the self-magnetic field exceeding the lower critical field. Contradicting this interpretation there are the temperature dependencies of the critical currents (fig. 14)), which seem to be closer to what one would expect from the local-heating model. But the local-heating model has one major problem with it, the presence of side peaks in contacts that are ballistic, where no local-heating should take place. With this in mind the interpretation based on the size dependencies of the critical currents seems more convincing.

If one accepts this explanation for the side peaks, then the thermodynamic critical field of Nb and the lower critical field of NbTi can be estimated from the measurements. From the slopes of the lines fitted into fig.(11) one gets 0.46 T for the thermodynamic critical field of Nb and 0.0023 T for the lower critical field of NbTi. The $B_{c,th}$ of Nb obtained in this way is more than twice the literature value of 0.2 T, meaning that this is probably not a very good way of measuring the thermodynamic critical field. The result for the lower critical field for NbTi is more reasonable, if not quite in line with literature values. Together with eq.(7) and the measured upper critical field of 12 T, the value of 0.0023 T for the lower critical field would result in a thermodynamic critical field of 0.16 T for the NbTi.

Lysykh et al. [19] have found the same linear dependance of the critical current on the contact radius for contacts between Cu and NbTi. The sizes of the contacts in their measurements were much larger with diameters roughly between 1 and 50 μm. The values of the critical currents in their measurements were very similar (when extrapolated to our contact sizes) to what was found in this study. While the experimental results are very much alike, their explanation for the cause of the side peaks is different: they argue that the side peaks are caused by the critical current density being exceeded (as is with Cu-Nb contacts in this study) and the linear dependance is caused by the current flowing on a thin ring on the periphery of the contact.

Earlier Naidyuk and Kvitnitskaya [20, cited in 1 p214], while studying contacts between Zr_2Ni and Cu, have found spectra similar to those described in this study as "Josephson-like". They were only found at low resistance contacts, the resistance dropped by more than a factor of two, the transition in the I-V curves was often discontinuous and the transitions were accompanied by a hysteresis. They found a linear relation between the critical current and the contact radius and attributed it to the self-magnetic field exceeding the lower critical field of the superconductor. They also argued that the reason this behavior is only seen in low resistance contacts, is because when the contact radius is less than the London penetration depth the movement of the normal state vortices becomes restricted.

Gloos, Huupponen and Tuuli [21] have proposed, that non-equilibrium phonons could cause broad side peaks at large bias voltages. They argue that applying a sufficiently high bias voltage generates non-equlibrium phonons, which can scatter the Andreev reflected holes, deflecting them from the contact. Those holes could then not be detected. This would reduce the total current flowing through the contact and would show up as a smooth maximum in the differential resistance spectra.

4.3 Sizes of the superconducting minima

In addition to the above discussion on the lack of a contribution from the vanishing Maxwell resistance, there is another question related to the sizes of the superconducting minima. In figure (17) there are many contacts where the resistance drops by a factor of more than two. Andreev reflection cannot explain this drop in their resistance. The behavior of the NbTi-NbTi (S-S) contacts can be attributed to the Josephson effect. With the N-S contacts there are two possibilities: the minima are the result of either the vanishing Maxwell resistances or the Josephson effect caused by the proximity effect inducing superconductivity in the normal metal. One problem with the vanishing Maxwell resistance, are the Nb contacts. As they are ballistic they should have no contribution from the Maxwell resistance and yet in some of them the resistance drops by more than a factor of two. Another problem shared by both of the explanations is the question of why the larger drops in resistances are only present in larger contacts.

One way this could be explained is to assume that there is a thin non-superconducting layer on the surface of the NbTi. In larger contacts the effect of this layer would be

negligible, as AR can still take place deeper in the superconductor and the contribution to the total Maxwell resistance from the thin layer is very small. In smaller contacts the portion of the total Maxwell resistance caused by the non-superconducting layer begins to grow and in sufficiently small contacts dominates the Maxwell resistance.

Another explanation has to do with the following observation [22]: When the zero bias resistances of large superconducting point contacts are measured as functions of the temperature, there is a sharp drop in the resistance at the critical temperature, much as if one would be measuring the bulk resistivity of the superconductor. If the contacts are made smaller the transition begins to broaden. It could be that at 4.2 K, where the measurements are made, the drop in the resistance is still incomplete resulting in much smaller superconducting minima.

Off course one could always argue, that the drops in the resistances are caused by the vanishing Maxwell resistances and that the contacts simply start being ballistic at resistances above 10 Ω or so. But doing so would effectively invalidate the results regarding the analysis of the side peaks, as those depend heavily on the conversions from resistances to radii.

As was with the discussion in 4.1 regarding the lack of the contribution from the vanishing Maxwell resistance, none of the possible explanations for the contacts laying between the ideal Josephson and the ideal AR lines in figure (17), can be easily proven or disproven. With this in mind it is best to consider the results of this part of this study as inconclusive.

Conclusions

We have found that the side peaks in the Nb and NbTi contacts can be attributed to two different mechanisms. In the Nb contacts they are caused by the critical current density of Nb being exceeded and in the NbTi contacts by the self magnetic field exceeding the lower critical field of NbTi. This seems like a convincing explanation for the causes of the side peaks, but the fact that the spectra of the NbTi contacts did not contain the kind of contribution from the vanishing Maxwell resistance that was expected based on the sizes of the contacts, casts very serious doubts on the validity of this explanation. The question as to why the vanishing Maxwell resistance of NbTi did not show up in the

spectra, is still an open one. Further study is needed to find an answer.

Acknowledgements

I would like to thank professor Kurt Gloos, the supervisor of this work, for his help, advice and patience. I would also like to thank professor Petriina Paturi and her group for letting me use their PPMS magnetometer and Matti Irjala for showing me how to use it. I also thank Yuri Naidyuk for his comments during the final stages of writing this thesis.

On a final note I should mention, that some of the measurements made for this thesis, were used in the ”Phonon-drag induced suppression of the Andreev hole current in superconducting niobium contacts” confrence paper [21] (26th International Conference on Low Temperature Physics) mentioned in 4.2.

References

[1] Yu. G. Naidyuk and I. K. Yanson, Point-Contact Spectroscopy (Springer Science, New York, 2005)
[2] Yu. V. Sharvin, Sov. Phys.-JETP 21 655 (1965)
[3] I. K. Yanson, Sov. Phys.-JETP 39 506 (1974)
[4] R. J. Soulen, J. M. Byers, M. S. Osofsky, B. Nadgorny, T. Ambrose, S. F. Cheng, P. R. Broussard, C. T. Tanaka, J. Nowak, J. S. Moodera, A. Barry and J. M. D. Coey, Science 282 85 (1998)
[5] F. Steglich, U. Rauchschwalbe, U. Gottwick, H. M. Mayer, G. Sparn, N. Grewe, U. Poppe, and J. J. M. Franse, J. Appl. Phys. 57 3054 (1985)
[6] N. Kohlrausch, Ann. Physik Leipzig 1 132 (1900)
[7] A. Wexler, Proc. Phys. Soc. (London) 89 927 (1966)
[8] M. Tinkham, Introduction to superconductivity (McGraw-Hill, New York, 1996)
[9] A. F. Andreev, Sov. Phys.-JETP 19 1228 (1964)
[10] R. D. Parks, Superconductivity Volume 2 (Marcel Dekker, New York, 1969)
[11] G. E. Blonder, M. Tinkham, and T. M. Klapwijk, Phys. Rev. B 25 4515 (1982)
[12] A. Pleceník, M. Grajcar, Š. Benacka, P. Seidel, and A. Pfuch, Phys. Rev. B 49 10016 (1994)
[13] I. I. Mazin, A. A. Golubov and B. Nadgorny, J. Appl. Phys. 89 7576 (2001)
[14] F. Pobell, Matter and Methods at Low Temperatures (Springer, New York, 2007)
[15] N. W. Ashcroft and N. D. Mermin, Solid State Physics (Harcourt, Orlando, 1976)
[16] M. T. Naus, R. W. Heussner, A. A. Squitieri and D. C. Larbalestier, IEEE Transactions on Applied Superconductivity 7 1122 (1997)
[17] B. W. Maxfield and W. L. McLean, Phys. Rev. 139 1515 (1965)
[18] T. P. Orlando and K. A. Delin, Foundations of Applied Superconductivity (Addison-Wesley, Reading Mass., 1991)
[19] A. A. Lysykh, G. V. Zasetsky and V. M. Bagatsky, Sov. J. Low Temp. Phys. 18 419 (1992)
[20] Yu. G. Naidyuk, O. E. Kvitnitskaya, Sov. J. Low Temp. Phys. 17 439 (1991)
[21] K. Gloos, J. Huupponen and E. Tuuli, Proceedings 26th International Conference on Low Temperature Physics (2011), http://arxiv.org/abs/1109.3770
[22] Yu. G. Naidyuk, K. Gloos and A. A. Menovsky, J. Phys. Cond. Matt. 9 6279 (1997)